ACS APPLIED MATERIALS & INTERFACES

Review

Cite This: ACS Appl. Mater. Interfaces XXXX, XXX, XXX−XXX

www.acsami.org

A Review of Micromotors in Confinements: Pores, Channels, Grooves, Steps, Interfaces, Chains, and Swimming in the Bulk

Zuyao Xiao, Mengshi Wei, and Wei Wang*

School of Materials Science and Engineering, Harbin Institute of Technology (Shenzhen), Shenzhen, Guangdong 518055, China

ABSTRACT: One of the recent frontiers of nanotechnology research involves machines that operate at nano- and microscales, also known as nano/micromotors. Their potential applications in biomedicine, environmental sciences and engineering, military and defense industries, self-assembly, and many other areas have fueled an intense interest in this topic over the last 15 years. Despite deepened understanding of their propulsion mechanisms, we are still in the early days of exploring the dynamics of micromotors in complex and more realistic environments. Confinements, as a typical example of complex environments, are extremely relevant to the applications of micromotors, which are expected to travel in mucus gels, blood vessels, reproductive and digestive tracts, microfluidic chips, and capillary tubes. In this review, we summarize and critically examine recent studies (mostly experimental ones) of micromotor dynamics in confinements in 3D (spheres and porous network, channels, grooves, steps, and obstacles), 2D (liquid−liquid, liquid−solid, and liquid−air interfaces), and 1D (chains). In addition, studies of micromotors moving in the bulk solution and the usefulness of acoustic levitation is discussed. At the end of this article, we summarize how confinements can affect micromotors and offer our insights on future research directions. This review article is relevant to readers who are interested in the interactions of materials with interfaces and structures at the microscale and helpful for the design of smart and multifunctional materials for various applications.

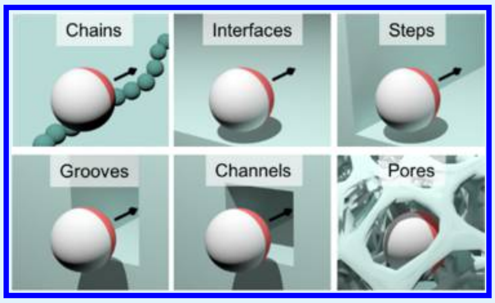

KEYWORDS: *interfaces, boundaries, self-electrophoresis, self-diffusiophoresis, acoustic levitation*

1. INTRODUCTION

One of the research frontiers of the rapidly advancing field of nanotechnology is the bottom-up assembly of machines at the micro- and nanoscale as well as demonstrations of their capability of manipulating other small-scale objects in a controlled and intelligent manner.[1] Driven by this ambition, decades of research have recently culminated in the recognition of molecular machines by the 2016 Nobel Prize[2] and the highly publicized international NanoCar race in 2017.[3,4] A couple of orders of magnitude larger, synthetic microswimmers capable of directional and spontaneous motion, also known as micromotors or colloidal motors,[5−11] represent a completely different approach to the "plenty of room at the bottom" vision.[12] These stimuli-responsive, biomimicry materials are certainly bulkier and less intricate than their molecular counterparts, but enjoy the benefit of being more powerful and easier to fabricate and visualize. They therefore hold considerable promises as the core platform for autonomous, multifunctional microrobotics of the next generation,[13−15] with applications spanning from minimally invasive surgeries[16] and drug delivery and biosensing[17] to environmental remediation,[18] defense and security,[19] and bottom-up assembly of micromachinery.[20]

To reach that bright future, however, there are hurdles to overcome, quite literally. Confinements, in the form of boundaries, interfaces, structural edges, and channels, are ubiquitous in natural and synthetic environments and are known to change the dynamics of colloidal particles undergoing Brownian motion via geometrical and hydrodynamic effects.[21−23] For instance, the mobility of particles could decrease with increasing temperatures, and their diffusion could even exceed the maximum diffusion limit.[24,25] Furthermore, the isotropic diffusion of Brownian colloids can be rectified into a directional migration if the confinements break symmetry.[21] The so-called Brownian ratchets are commonly employed in many biological systems to produce directional transport from random diffusion,[26,27] and microfabricated asymmetric structures, such as pores or channels, were shown to be capable of rectifying Brownian colloids as well.[28−30]

Microswimmers, natural or synthetic, are motile and therefore able to probe much larger areas than Brownian particles and are thus more prone to encounter microstructures that block the way. In addition, because they are typically not density-matched to their surrounding medium, microswimmers inevitably sediment to the bottom or float to the liquid−air interface, both of which induce strong boundary effects (see Section 3.2 for a detailed discussion). Besides having a strong influence on the dynamics of natural microorganisms,[31−38] confinements are especially important to synthetic micro-

Received: August 1, 2018
Accepted: December 18, 2018
Published: December 18, 2018

DOI: 10.1021/acsami.8b13103
ACS Appl. Mater. Interfaces XXXX, XXX, XXX−XXX

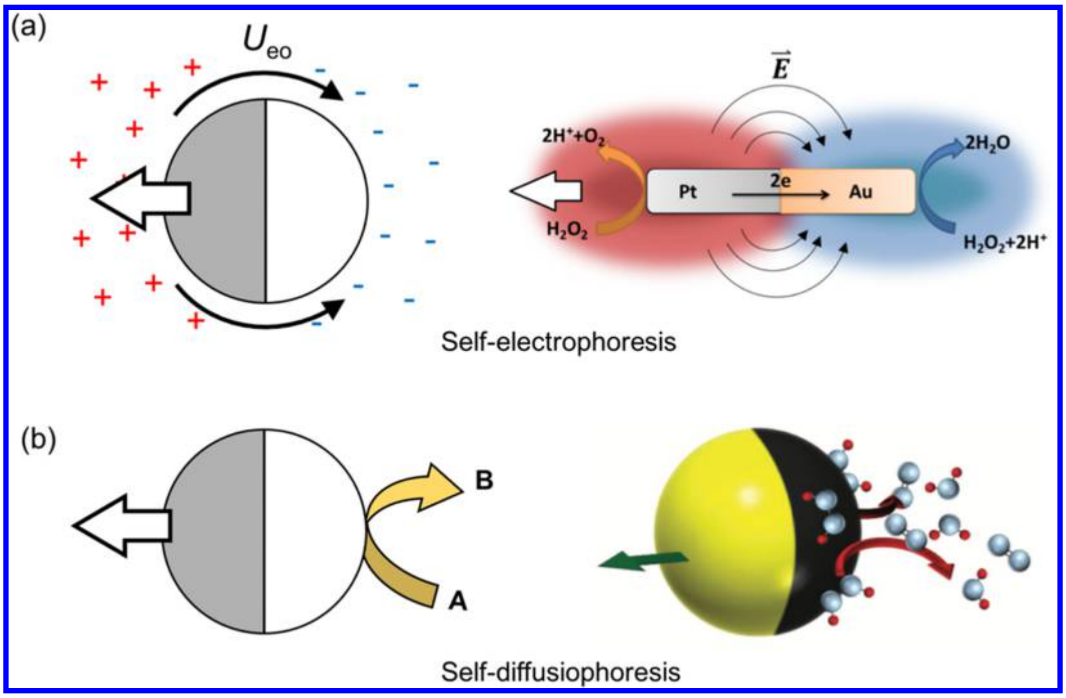

Figure 1. Micromotors powered by self-generated chemical gradients. (a) Self-electrophoresis. Left: a generic case, where U_{eo} is the electroosmotic velocity. Right: a gold−platinum (Au−Pt) microrod moving in H_2O_2 as a specific example of self-electrophoresis. Reprinted with permission from ref 113. Copyright 2013, American Chemical Society. (b) Self-diffusiophoresis. Left: a generic case, where species A is chemically converted to B. Right: As a specific example of self-diffusiophoresis, a polystyrene (PS) microsphere half-coated with Pt moves by catalyzing the decomposition of H_2O_2 into H_2O and oxygen.[56] Reprinted from ref 56 which is licensed under CC BY 4.0.

motors for fundamental and applied reasons because many of their proposed applications involve moving through narrow passages such as viscoelastic gels,[39] blood vessels,[40−43] reproductive and digestive tracts,[44,45] and microfluidic chips.[46−49] Not only do confinements physically limit how the micromotors are populated and where they go, but more importantly, the complicated interplay among hydrodynamics, electrostatics and electrokinetics, and transport of chemical species can alter the behaviors of micromotors tremendously.

Although recent studies have begun to explore the critical effects of confinements on micromotors,[50−53] our systematic understanding of this topic is still quite limited. In this review article, we summarize the latest progress of discovering and understanding how micromotors (especially those powered by chemical gradients) are affected by confinements, with a particular emphasis on experimental studies. To complement this topic, we also review the limited amount of studies on the dynamics of micromotors moving in the bulk solution (i.e., absent of boundaries and confinements) and discuss a few techniques useful for studying micromotors in the bulk. Finally, we summarize the four ways in which confinements can affect micromotors (physically, hydrodynamically, electrostatically, and electrokinetically) and comment on what is missing in the current research and promising research prospects. Although there are plenty of review articles on the emerging field of micromotors, this one focuses on a specific topic: how micromotors interact with a confining environment. We tried our best to write this article in a way that is easily approachable and friendly to scholars and students from other research areas while at same time offering necessary information, critical comments, and forward-looking insights to everyone interested in this topic. In doing so, we hope this review article can help the scientific community, especially young researchers, identify key scientific questions, and serve as a roadmap that guides micromotor research toward more exciting discoveries.

2. CHEMICAL PROPULSION OF MICROMOTORS: A QUICK OVERVIEW

Before we begin our discussion on micromotors moving in confinements, it is perhaps helpful, especially to readers outside this research field, to briefly introduce the propulsion mechanisms of micromotors. In particular, we explain two types of propulsion that are both related to self-generated chemical gradients (see Figure 1),[8] because motors driven by these two mechanisms are not only the primary subjects in the following discussions but also among the most popular micromotors studied so far. These micromotors often employ so-called "Janus" structures that break symmetry and induce asymmetric chemical gradients.[54,55]

The first type of micromotor is bimetallic microrods that move in H_2O_2 solutions (Figure 1a), which have been studied extensively since the beginning of micromotor research roughly 15 years ago.[57] As a result, its propulsion mechanism has been understood reasonably well, which is very helpful for further understanding of how these micromotors interact with others as well as confinements. The propulsion mechanism, termed self-electrophoresis, originates from a bipolar electrochemical decomposition of H_2O_2 occurring on both ends of the microrod.[58] The anodic and cathodic ends produce and consume protons during the reaction, respectively, and together generate a proton gradient and therefore an electric field. The charged microrod moves in its self-generated electric field toward the anode end, in a way similar to electrophoresis. Other self-electrophoretic micromotors that rely on different surface reactions and transport of ions beyond protons have also been reported in recent years.[59−63]

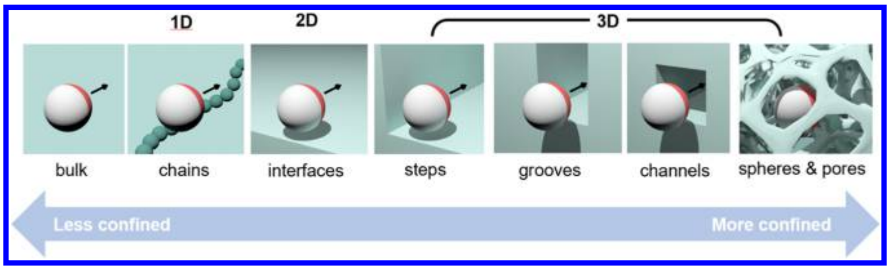

Figure 2. Classification of confinements. Depending on the degrees of geometrical confinement, different structures and boundaries can be categorized into 3D (including spheres and porous network, channels, grooves, and steps), 2D (interfaces), and 1D (chains). A micromotor moving in the bulk in the absence of confinements is illustrated on the left for comparison. An arbitrary Janus micromotor is drawn for illustrative purpose only and is not necessarily to scale with the size of the confinement.

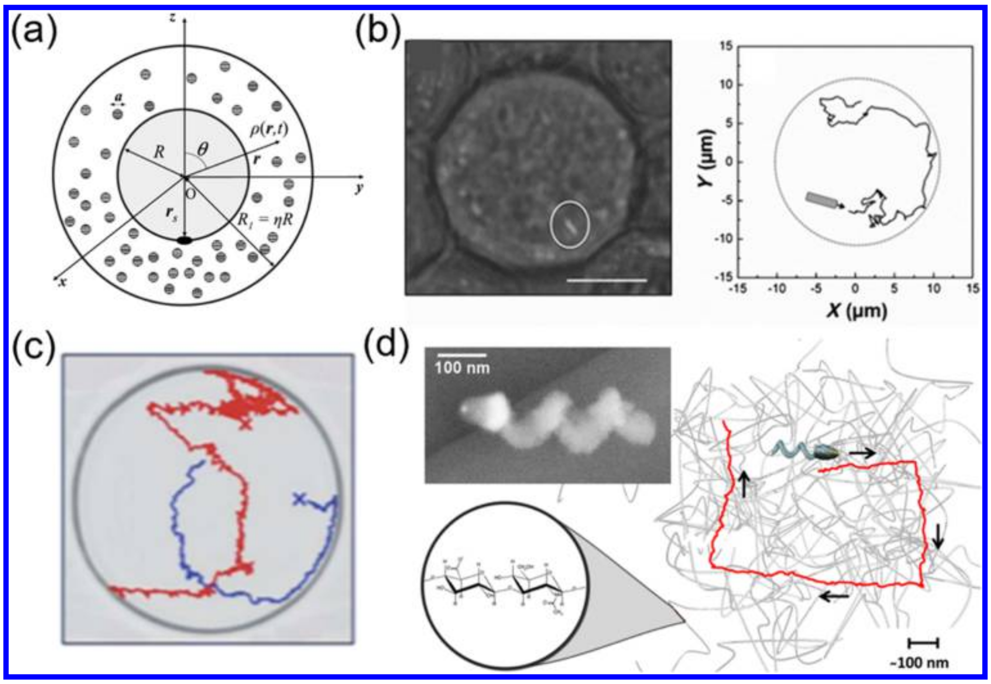

Figure 3. Micromotors confined by spheres and porous networks. (a) Theoretical study of a self-diffusiophoretic micromotor confined in an impermeable spherical shell. Reprinted with permission from ref 83. Copyright 2009, John Wiley and Sons. (b) Metallic microrods confined inside a living HeLa (human cervical cancer) cell and activated by ultrasound. Left: an optical micrograph with the microrod circled. Scale bar: 10 μm. Right: a representative trajectory of a microrod moving inside a HeLa cell. Reprinted with permission from ref 84. Copyright 2014, John Wiley and Sons. (c) Experiment (red) and simulated (blue) trajectories of a 2.13 μm Janus micromotor moving in a circular confinement. Reprinted with permission from ref 85. Copyright 2011, CCC Republication. (d) A helical nanopropeller powered by rotating magnetic fields moves through a porous hyaluronan gel. Reprinted with permission from ref 39. Copyright 2014, American Chemical Society.

The other popular mechanism, termed self-diffusiophoresis, also powers micromotors by a chemical reaction that occurs asymmetrically on the particle surface (Figure 1b).[64−67] But instead of splitting the reaction into anodic and cathodic half reactions that occur on separate ends, the chemical reaction occurs only on one side of a Janus particle. This mechanism can be further divided into ionic or nonionic diffusiophoresis depending on the nature of the reaction products. In ionic diffusiophoresis, the ionic products diffuse at different rates, generating an electric field that couples to the particle surface charges and induces electrokinetic flows that propel the particle.[68] In nonionic diffusiophoresis, however, it is the difference in the interaction between the product molecules and the particle surface that determines the strength and directionality of propulsion. Popular examples of self-diffusiophoretic micromotors include Pt-coated dielectric microspheres in H_2O_2,[69,70] photoactive TiO_2 and AgCl Janus particles,[68,71−74] and many enzyme-powered Janus micromotors.[75−77] However, it is important to note that the exact mechanisms of these micromotors mentioned above, especially those involving Pt or TiO_2 Janus particles, remain controversial,[78,79] partly because of the experimental difficulty in identifying intermediate species.

The dynamics of self-electrophoretic or diffusiophoretic micromotors are dominated by a complicated interplay among surface chemical reactions, transport of chemical species, low Reynolds number hydrodynamics (Stokes flow), electrostatics, and/or electrokinetics. Because these processes are all sensitive to the local environment as well as the nature of confinement, it is reasonable to expect these types of micromotors to experience some of the strongest confinement effects that will be discussed extensively in the following sections.

There are certainly many other means to power micromotors. For example, a popular chemical method exploits the release of oxygen bubbles from fast catalytic decomposition of H_2O_2 by materials such as Pt or MnO_2. Oxygen bubbles are

DOI: 10.1021/acsami.8b13103
ACS Appl. Mater. Interfaces XXXX, XXX, XXX−XXX

generally only produced from one side of the particle and therefore push it away via a recoil mechanism.[80] External fields such as electric field, magnetic field, light, or ultrasound can also exert forces on colloidal particles in various ways and therefore have been used as power sources provided that symmetry is broken somehow.[81,82] However, these propulsion mechanisms are not the main subject of this current review, and interested readers are directed to related review articles.

3. MICROMOTORS IN CONFINEMENTS

It is somewhat daunting to imagine all the different ways for a micromotor to be confined, with various confinement geometries, interaction mechanisms, and outcomes. To streamline our discussion, and as an attempt to unify the terminology, we identified and grouped various types of structures and boundaries that confine micromotors in three, two, and one dimensions (3D, 2D, and 1D) into six categories. Illustrated in Figure 2, 3D confinements include, in the order of decreasing degrees of confinement, porous networks and spheres, channels, grooves, and steps. 2D confinements are typically interfaces where micromotors are trapped. 1D confinement is rare, and the only reported example is microchains in solution that direct micromotors. For comparison, we also illustrated a micromotor moving in the bulk solution, which will be discussed in Section 4 of this review article. In the following discussion, we progress as the degree of confinement decreases and examine how a micromotor changes its behavior as its shackles are gradually loosened.

3.1. 3D Confinements. *Motors in Spheres.* We start with the strongest confinements, which limit micromotors from all directions. A micromotor can of course be trapped in a solid and rendered motionless because of extreme confinements, but it can hardly be called a micromotor, and therefore its usefulness disappears. Taking this extreme case one notch down would be to allow a micromotor a small amount of freedom and some room to move, and one such scenario is micromotors in a small, isolating spherical shell. For example, Popescu et al. theoretically studied the dynamics of a diffusiophoretic micromotor placed in a concentric, impermeable, spherical shell of solution (Figure 3a).[83] They showed that, despite an increase in viscosity as a result of the nearby no-slip boundaries, the presence of a confining wall also leads to a significant increase in the velocity of the self-propelled particle, primarily because of an increase in solute concentrations. Experimental realization of "motors in a sphere" scenario, however, is scarce, with only a few studies attempting to explore motor dynamics in a somewhat tight sphere. For example, Wang et al. internalized gold microrods (3 μm long and 300 nm in diameter) inside living HeLa cells (~20 μm in diameter) and observed their motion along the cell membrane when activated by ultrasound (Figure 3b).[84] Similar trajectories were found for 2.13 μm Janus micromotors swimming in a circular well 38 μm in diameter (Figure 3c).[85] The confinements in these studies are clearly far from being 3D or tight.

Such an experiment has been challenging for obvious reasons. Chemically powered micromotors consume and produce chemicals, and either the buildup of unwanted products (such as oxygen) or the consumption of fuels (such as enzyme substrates or H_2O_2) would soon cause problems for the continuous operation of the motors in a tightly confined space. Membranes permeable to the transport of these chemicals would in principle mitigate this problem, but this is yet to be demonstrated. On the other hand, micromotors actuated via external fields such as electric field, magnetic field, light, or ultrasound do not face the mass transport problem and are perhaps better candidates for studies of strong confinements, provided that they can be trapped within droplets of an appropriate medium with sizes comparable to motor dimensions (typically smaller than a few micrometers). To move beyond physical boundaries, we can further imagine three-dimensional potential traps within which a micromotor is allowed to move. This could potentially be achieved by acoustic levitation or optical tweezers, which are further discussed in Section 4.2.

Motors in Porous Networks. A second type of complex environment confining micromotors from all directions is porous networks such as gels, which are widely found in biological media. To prove the viability of using micromotors for biomedical applications such as drug delivery or microsurgery, it is particularly important to prove and understand their propulsion dynamics in porous media. A previous body of literature has shown that the dynamics of a biological microswimmer in such an environment is highly dependent on the swimmer shape and size as well as the intrinsic properties of the media such as their pore sizes.[86−88] Building upon this knowledge, a number of recent experiments studied the operation of synthetic micromotors in porous media. In 2014, Schamel et al. demonstrate that helical nanopropellers can be controllably steered through hyaluronan (Figure 3d).[39] This gel media is widely found in the human body (especially in joints and eyes), and previous studies have shown that larger microswimmers (~400 nm) could not propel in such a densely meshed network. The pleasant surprise in this report is that nanoscrews as small as 70 nm not only moved in hyaluronan, but even at a higher speed than in Newtonian fluids. This was attributed to an enhanced propulsion efficiency for smaller nanopropellers. In another creative study with magnetically propelled nanohelices, Walker et al. showed that they moved through gastric mucin gels by making use of surface-immobilized urease.[89] This was inspired by bacteria *Helicobacter pylori*, which produces urease that raises local pH and liquefies mucus via a gel−sol transition to allow itself to move. From an application perspective, this biomimetic micromotor is potentially useful as a drug carrier that can efficiently deliver drugs across the mucosal barriers in the gastrointestinal tract. However, one has to consider whether the enzymatic coating and the loaded drugs interfere with each other, and how exactly the drugs are unloaded. We also briefly note that interesting dynamics of micromotors in viscoelastic but not confining environments have also been reported, including a strong coupling of rotational to translational diffusion coefficient,[90] abnormal scaling between motor speeds and its driving force,[91] and the breakdown of the so-called "scallop theorem".[92]

Micromotors in Narrow Channels. A great many applications require micromotors to move in/near artificially constructed structures or features, such as microfluidic channels, stripes of electrodes, lithographic patterns, or larger particles. Although the degree of confinement in these cases becomes smaller than the previously discussed scenarios, its effect is still far from being negligible.

We begin with tight but generally straight channels/pores with width and height slightly larger than the size of a micromotor, which is allowed to move freely along the channel

DOI: 10.1021/acsami.8b13103
ACS Appl. Mater. Interfaces XXXX, XXX, XXX−XXX

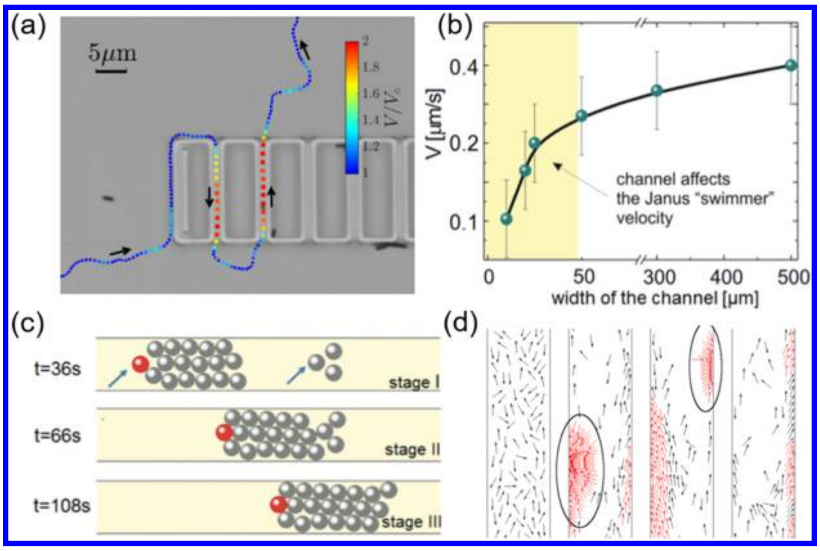

Figure 4. Micromotors in tight channels. (a) Self-electrophoretic bimetallic microrod doubles its speed in a tight channel comparable to its size. Reprinted with permission from ref 94. Copyright 2016, American Physical Society. (b) $Pt-SiO_2$ micromotor significantly slows in confining channels. (c) A $Pt-SiO_2$ micromotor moves forward collectively with nearby tracer particles in a channel. Reprinted with permission from ref 95. Copyright 2016, John Wiley and Sons. (d) Simulation results of self-propelled rods aggregating into clusters in microchannels. Reprinted with permission from ref 96. Copyright 2008, American Physical Society.

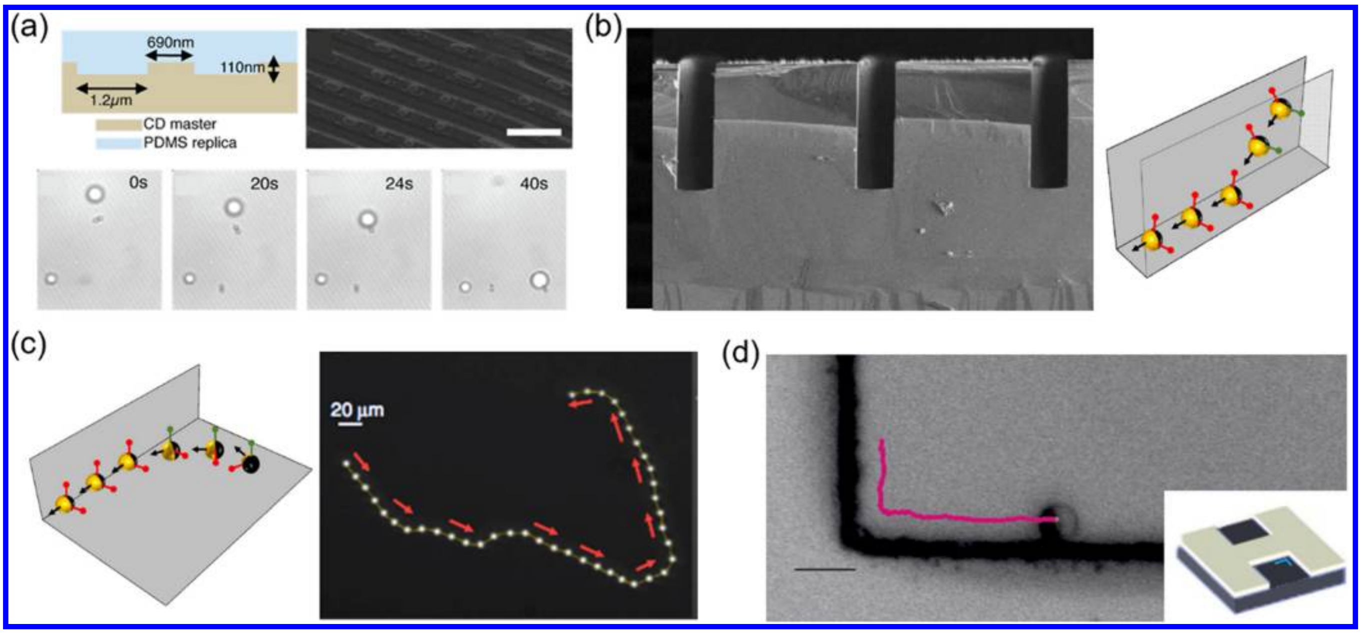

Figure 5. Micromotors moving in grooves and near steps. (a) Hematite microparticles attract tracer particles into dimer that moves along prefabricated microgrooves. Top: schematics of the grooves and a scanning electron micrograph. Scale bar: 2 μm. Bottom: time-elapsed optical micrographs showing the motion of hematite−tracer dimers along grooves. Reprinted with permission from ref 97. Copyright 2013, American Chemical Society. (b) Janus micromotors moving in a deep trench. Left: a scanning electron micrograph of the fabricated trenches (∼37 μm deep). Right: schematic showing how the Janus motor moves in a trench. (c) Janus micromotors moving along a step. Left: schematics. Right: overlaid optical micrographs of a 1.55 μm Janus particle moving at the bottom of a rectangular glass cuvette along its edge. Reprinted from ref 98, which is licensed under CC BY 4.0. (d) A Janus particle tracked while maneuvering around a 90° corner. Scale bar: 10 μm. Inset: schematic of the microfabricated structure. Reprinted from ref 99, which is licensed under CC BY 4.0.

length but confined in the other four sides (top, bottom, left, and right). Although tight channels commonly slow biological microswimmers due to hydrodynamic effect (i.e., no-slip boundaries),[31−38] their effect on synthetic microswimmers is more complicated. For one, the speeds of micromotors could increase or decrease depending on the property of motors and channels. For example, Yang et al. numerically simulated the self-diffusiophoresis of Janus catalytic micromotors in a tight micropore via an arbitrary Lagrangian−Eulerian (ALE) method.[93] They discovered that such micromotors moved more slowly than in the bulk, yet they maintained a steady orientation thanks to their interaction with the channel. Such a decrease in motor speed was attributed to an interplay between hydrodynamics and a chemical effect, but possible electrokinetics at the pore wall was not considered in their model. Electrokinetic effect, however, was found in two separate

DOI: 10.1021/acsami.8b13103
ACS Appl. Mater. Interfaces XXXX, XXX, XXX−XXX

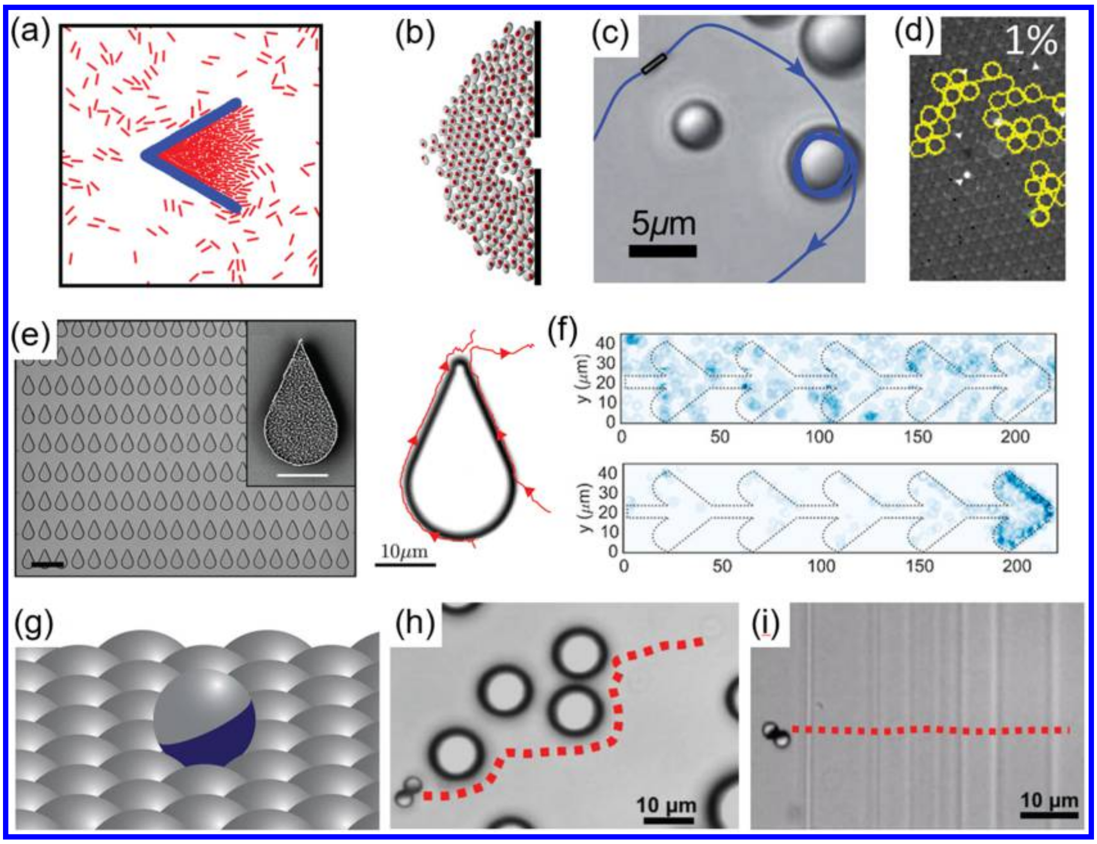

Figure 6. Micromotors near obstacles. (a) Simulation of trapping of micromotors by wedge-shaped obstacles. Reprinted with permission from ref 100. Copyright 2013, American Physical Society. (b) Simulation of self-propelled rods moving through a bottleneck. Reprinted from ref 102, which is licensed under CC BY 4.0. (c) Bimetallic micromotor orbits around a large polystyrene microsphere. Reprinted with permission from ref 103. Copyright 2014, CCC Republication. (d) Trajectories of Pt-coated Janus micromotors moving through a closed packed monolayer of 10 μm polystyrene microspheres. Reprinted from ref 104, which is licensed under CC BY 4.0. (e) Left: an optical micrograph of microfabricated teardrop-shaped structures, scale bar 50 μm (inset: an SEM image, scale bar 10 μm). Right: trajectory of a micromotor moving along a teardrop-shaped structure. Reprinted with permission from ref 106. Copyright 2017, CCC Republication. (f) Average positions of micromotors in a linear ratchet channel at t = 0 s (top) and 60 s (bottom), showing an accumulation of micromotors over time at one end of the channel. Reprinted with permission from ref 107. Copyright 2014, American Chemical Society. (g) Schematic of a Janus micromotor moving on top of a colloidal crystal. Reprinted from ref 109, which is licensed under CC BY 4.0. A magnetic microdimer moves around large microspheres (h) and across multiple scratches on the surface (i). Reprinted with permission from ref 110. Copyright 2018, John Wiley and Sons.

studies to be critical for chemically driven micromotors in a tight channel. In one study, Liu et al. experimentally investigated bimetallic microrods (a few micrometers in length and 300 nm in diameter) in linear and curved channels that were fabricated by direct laser writing (Figure 4a) and had heights and widths slightly larger than those of the microrods.[94] They found that motors moved up to 5 times faster inside the channels than outside, and such a speed increase was largely independent of solution conductivity or fuel (H_2O_2) concentrations. Numerical simulation revealed that the confinement increased the strength of the self-generated electric field which was driving the motor forward. In addition, the electroosmotic backflow from the charged channel wall further helped the motor to move faster. In a second study, however, SiO_2−Pt Janus micromotors were found to move more slowly in a tight channel with a width about 10 times that of the particle diameter (Figure 4b).[95] The authors proposed that the motor slowed possibly due to a tendency to hit and move along the wall as well as an implicit motor−wall interaction. The discrepancy between these two reports is interesting and is perhaps related to the difference between their propulsion mechanisms (microrods move by self-electrophoresis, whereas Janus Pt motors move, arguably, by diffusiophoresis).

The situation becomes more complicated when more particles are present in the channel. In one example, a SiO_2−Pt Janus micromotor can collect many passive tracer particles and lead to clogging of the channel, where the whole assembly moves forward (Figure 4c).[95] In addition, Wensink and Lowen showed in a simulation that self-propelled rods, when moving in a channel, first grew to hedgehog-like clusters, which then dissolved into nematized motile aggregates that slid past the walls (Figure 4d).[96] Considering the complicated interactions between the motor and the channel, it is natural to expect rich dynamics and interesting collective behaviors to emerge for systems of large number density. This remains an interesting frontier for future exploration and will be briefly discussed again at the end of this article.

Motors in Grooves. Long, shallow cuts on a surface, also known as grooves, pose three-direction restrictions on the movement of the motor from both sides and the bottom, while they are free to move along the length. Interesting, although motors are also free to escape from the uncovered top into the bulk solution, they almost never do that (notable exceptions are antigravitactic micromotors), but instead tend to be

DOI: 10.1021/acsami.8b13103
ACS Appl. Mater. Interfaces XXXX, XXX, XXX−XXX

attracted to the groove sidewalls or its bottom. Such a striking preference is repeatedly observed in many reports with 3D structures and seems to be a robust feature for micromotors powered by chemical gradients. For example, Palacci et al. used polydimethylsiloxane (PDMS) to fabricate patterns that consisted of grooves that were 1.2 μm wide and 110 nm in height (Figure 5a).[97] Upon turning on the light, peanut-shaped hematite microparticles aligned along the grooves and phoretically attracted a polymer microsphere into a dimer that moved along the groove sidewalls. In another study, Das et al. lithographically fabricated an array of deep rectangular grooves (~8 μm wide and ~40 μm deep) and found that the strong confinement coming from three surfaces leads to a strictly linear motion of Pt-coated polystyrene spheres in the grooves with few or no "Brownian escapes" (Figure 5b).[98]

Although very few recent studies have focused on the dynamics of micromotors in grooves, their unique structures present fertile grounds for many future studies. For example, one might wonder how a micromotor sinks inside a deep groove, confined by two sides, but with an ever-closer bottom that both hydrodynamically and electrokinetically couples to the sedimenting motor. Similarly, the recent discovery of antigravitactic motors that move upward and against gravity could also be significantly affected when moving in a deep trench (see later discussions). Finally, micromotors moving in grooves could easily line up into a series of moving particles, whose collective dynamics remain an interesting question.

Motors near Steps. Steps are 3D structures that confine micromotors from two directions (one sidewall and at the bottom). Micromotors moving near a step often attract to the side wall and are rectified into a directional motion along the edge. This is particularly noticeable for micromotors moving near vertical sidewalls that are significantly taller than the motor. For example, Das et al. observed that a Janus micromotor initially exhibiting 2D-enhanced diffusion at a bottom surface transitioned into linear motion when it reached the vertical edge of a cuvette (Figure 5c).[98] Simmchen et al. demonstrate that step-like submicrometer topographical features can be used as reliable docking and guiding platforms for chemically active spherical Janus colloids, as shown in Figure 5d,[99] possibly due to a change in chemical activity and associated hydrodynamic effect.

This study by Simmchen et al. also highlights an important feature of steps: whether a micromotor can be captured by a step is very sensitive to its height relative to the motor size, and as the height of the step decreases, it is easier for the micromotor to cross. One naturally wonders if such a scaling can be explained more quantitatively, and how additional parameters of the steps, such as their shapes and surface features, would affect the micromotors moving nearby. A naïve guess would be that a micromotor overcoming an obstacle follows a Boltzmann-like probability distribution, where a higher energy barrier becomes exponentially more difficult to surmount. But details of the motor−wall interaction could easily break this hypothesis, and existing experimental data (such as those found in Figure 5 of ref 99) are too crude to draw any conclusion. Experimental investigation of these questions that are important for using micromotors in realistic environments remains largely unexplored.

Motors near Obstacles. As the height and sizes of a step decrease, it reduces to microscale structures that are still able to attract micromotors at the edges and guide their motion. There, depending on the geometry of the structures, referred to as "obstacles", micromotors can be collected at a particular spot of sharp concavity, trapped into orbiting trajectories, or rectified to move in a certain direction. For example, Kaiser et al. and Restrepo-Pérez et al. independently studied by simulation and experiments, respectively, how chevron-shaped obstacles can trap active particles (Figure 6a).[100,101] Clogging of micromotors could also occur near an opening, and Parisi et al. numerically investigated the interesting question of how active particles flow through a bottleneck (Figure 6b).[102] Counterintuitively, they found that clogging at the exit was worse when particles propelled along their long axis and therefore formed more ordered structures at the bottleneck. Particles propelling without any preferred orientation, on the other hand, maximized the outflow through a bottleneck. This is perhaps important for using micromotors in scenarios of drastically changing confinements, such as microbots entering capillaries from arteries.

Besides being trapped or clogged near a point, micromotors could also be trapped into an orbital trajectory due to their preference of following an edge. Takagi et al. showed that chemically propelled microrods can be captured, with little change in their speed, into tight orbits around large tracer microspheres on a bottom substrate (Figure 6c).[103] Similar observations were also made by Brown et al. with Pt−PS Janus micromotors near larger microspheres (Figure 6d).[104] In both cases, the capturing of micromotors by larger spheres was believed to be due to hydrodynamic interactions.

Because micromotors tend to follow obstacles, their asymmetric shapes provide an opportunity to rectify motor trajectories. Chen et al. simulated nanoswimmers in a channel with a strip of funnel gates,[105] where obstacles of various geometries and curvature were found to rectify motor trajectories via geometry-assisted diffusion or trap-hindered diffusion. Teardrop-shaped posts were also found to rectify micromotors, which preferentially depart from the high curvature end (Figure 6e).[106] Similar principles can also be applied to ratchet-shaped channels (Figure 6f).[107] An interesting consequence of rectification by asymmetric shapes is sorting. Mijalkov et al. demonstrated by numerical simulations how the chirality of circular motion could couple to chiral features present in the microswimmer environment.[108] Chiral microswimmers can therefore be sorted on the basis of chirality, linear velocity, and angular velocity of their motion.

Shallower obstacles can also serve as energy barriers that regulate the diffusion of micromotors on an otherwise flat and energetically uniform surface. This was recently demonstrated by Choudhury et al., who studied both experimentally and theoretically the dynamics of chemically self-propelled Pt−SiO_2 Janus colloids moving on a periodic surface (Figure 6g).[109] The surface is a close-packed monolayer of SiO_2 microspheres, which acts as a periodic trapping potential. Interestingly, depending on the relative strength of motor activities (tuned by H_2O_2 concentrations) and that of the trapping potential (fixed by geometry, but potentially tunable via surface functionalization), the long-time diffusion of micromotors can be either enhanced or suppressed. This finding, the authors argue, can be generalized to many other micromotor systems.

As the size of obstacles continues to decrease, they are eventually unable to physically block micromotors that are large and powerful. This is especially true for micromotors powered by external fields such as magnetic fields, because the

DOI: 10.1021/acsami.8b13103
ACS Appl. Mater. Interfaces XXXX, XXX, XXX−XXX

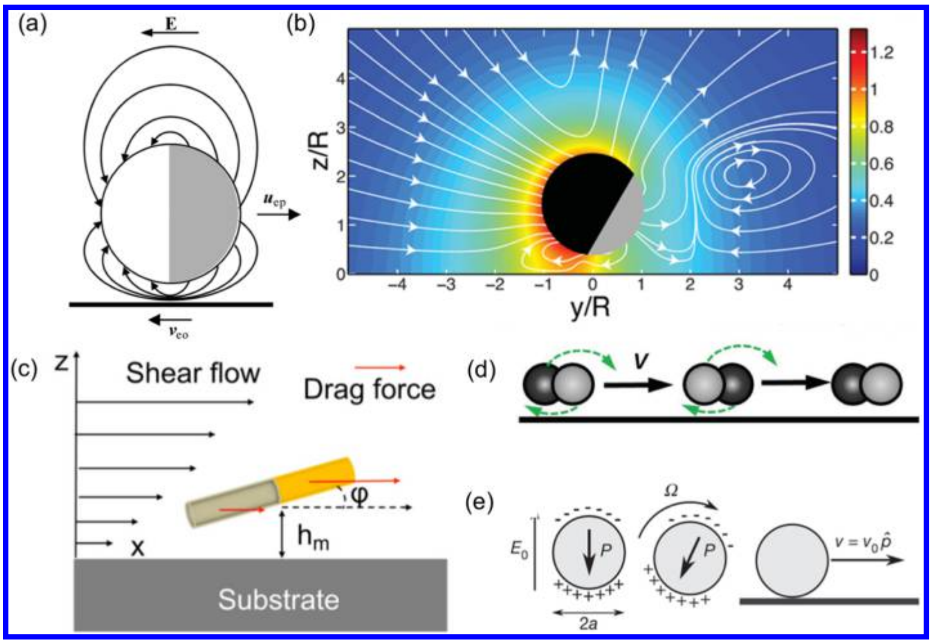

Figure 7. Micromotors moving near a solid−liquid interface. (a) Self-electrophoretic Janus micromotor moving to the right experiences two effects from the bottom substrate: a squeezed electric field and a counter-acting electroosmotic flow. Reprinted with permission from ref 112. Copyright 2014, American Chemical Society. (b) Fluid flow (white streamlines) and solute concentrations normalized by bulk concentration (color legend) of a gliding Janus micromotor near a bottom substrate. Reprinted with permission from ref 118. Copyright 2014, CCC Publication. (c) A chemically powered bimetallic microrod moves upstream (rheotaxis) by tilting in a shear flow. Reprinted with permission from ref 123. Copyright 2017, American Chemical Society. (d) A magnetic dimer moves in an AC magnetic field gradient by alternating two spheres forward near a bottom substrate. Reprinted with permission from ref 110. Copyright 2018, John Wiley and Sons. (e) Quincke rollers move on a bottom substrate when polarized by a DC electric field. Reprinted with permission from ref 130. Copyright 2013, Springer Nature.

tendency to follow edges due to chemical gradients or phoretic effects is eliminated. This was recently demonstrated by Li and Zhang et al., where a magnetic microdimer that walks on a substrate in an alternating magnetic field could nudge its way through a crowd of microsphere obstacles or even walk over shallow cracks on the surface (Figure 6h, (i).[110] As noted above, it would be interesting to systematically study how the shapes and sizes of an obstacle affect its interaction with a nearby micromotor, as well as to find the threshold height below which the motor is no longer considered to be confined.

3.2. 2D Confinements. *Motors on Solid−Liquid Interfaces (Walls).* Given that most artificial microswimmers are made of materials of higher density than the liquid medium (typically water), they naturally sediment to the bottom of the observation chamber or devices, where they interact with a solid−liquid interface (also referred to as a wall). In many cases, this wall is made of glass (SiO_2) of negative surface charges. The presence of a flat wall can therefore significantly affect the speeds of a nearby micromotor via hydrodynamics, a distortion of electric fields, or electroosmosis. Whether the wall is inert or actively participates in generating electrokinetics becomes critical. Using lattice Boltzmann simulation, Shen et al. studied the interaction between a Janus micromotor and an inert wall. Interestingly, it was found that motor could be hydrodynamically trapped to the surface, and while trapped, its speed is higher than when moving in the bulk.[111] When propulsion details are considered, however, the dynamics change completely. Chiang et al. simulated how the speed of a self-electrophoretic micromotor changes with its distance from a charged wall. Although the self-generated electric field is "squeezed" by the confinement from the bottom, the localized electroosmotic flows from the wall reduced motor speeds by 25% when experimental values were concerned (Figure 7a).[112] Such a speed decrease was qualitatively supported by experiments with bimetallic microrods moving on glass,[113,114] and electroosmotic flows are believed to be also able to reverse the direction of tadpole-shaped SiO_2−TiO_2 micromotors depending on their sizes and shapes.[115] In some cases, the presence of the wall can even actuate the motor that is not moving: while chemically active homogeneous spherical particles do not undergo self-diffusiophoresis in free solution, they may do so when suspended in the vicinity of a solid boundary.[116] This was also demonstrated with hematite microparticles that "surf" on charged bottom surface, presumably due to electroosmotic flow and local symmetry breaking.[117] Furthermore, as mentioned in a previous discussion, a charged wall and its electroosmosis can also speed up micromotors if they are confined very strongly.[73]

Walls can also modify the orientation of micromotors, leading to rich dynamics. For example, a theoretical study by Uspal et al. revealed that self-diffusiophoretic Janus micromotors could reflect from, hover at, or slide along a nearby wall, depending on the surface coverage of the Janus micromotor and its mobility (Figure 7b).[118] Similar results were reported theoretically by Mozaffari et al.[119] These interesting dynamics, which remain to be confirmed by experiments, are primarily due to modified chemical gradients in the presence of confining walls, although it has been reported that pure physical reasons can also reorient an L-shaped micromotor moving in circles and close to a boundary.[120] In an attempt to separate the contributions of hydrodynamics and distortion of chemical gradients to micromotor dynamics, Ibrahim and Liverpool concluded that, for a diffusiophoretically propelled micromotor, the

DOI: 10.1021/acsami.8b13103
ACS Appl. Mater. Interfaces XXXX, XXX, XXX−XXX

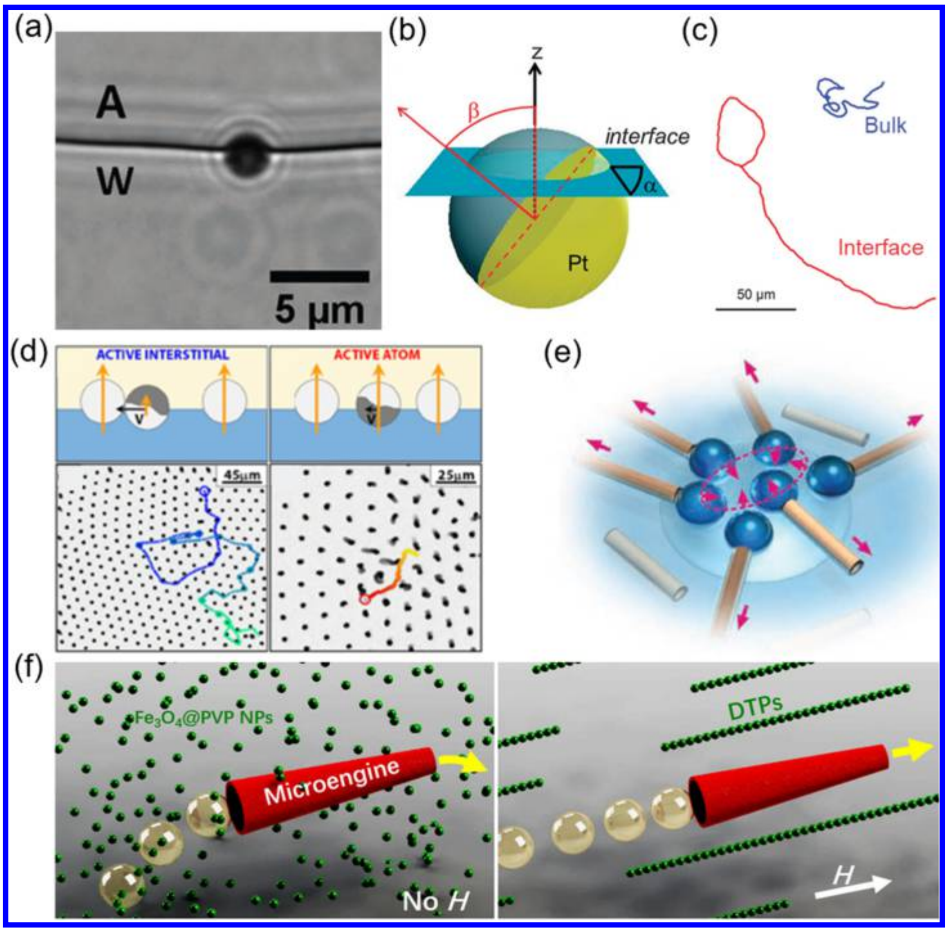

Figure 8. Micromotors moving on liquid−air interfaces (a−e) and near chains (f). (a−c) Optical micrograph (a), schematic (b), and trajectory (red in c) of a Pt-coated Janus micromotor moving on the air−water interface. Its trajectory of moving in the bulk is given in blue in (c) for comparison. Reprinted with permission from ref 134. Copyright 2015, CCC Publication. (d) Depending on its orientation, a Janus micromotor on a water−hexadecane interface can move within the interstices of a colloidal crystal (left) or push microspheres in the crystal around (right). Reprinted with permission from ref 136. Copyright 2018, American Physical Society. (e) Schematic of an aggregation of bubble-propelled microtubes by a capillary effect. Reprinted with permission from ref 137. Copyright 2010, John Wiley and Sons. (f) Schematic of the motion of a bubble-propelled microtube in ferrofluid before (left) and after (right) applying a magnetic field. DTP stands for dynamic topographical pathways. Reprinted with permission from ref 148. Copyright 2018, American Chemical Society.

wall-induced-diffusiophoresis effect increases motor speed, while hydrodynamic effects could either attract or repel motors from the wall.[121] Furthermore, Volpe et al. found that when a self-propelled particle hits an obstacle such as a planar wall, the force can be decomposed into two components: one tangential and one normal to the wall. The tangential component will lead to sliding along the wall, while the normal component will be compensated by the steric wall−particle interaction.[122] The reorientation of micromotors near a bottom wall, when coupled to an external flow, can lead to rheotaxis of rod-shaped micromotors. This was demonstrated in a recent experimental study by Ren et al., where a bimetallic microrod fueled by H_2O_2 and operating in self-electrophoresis was aligned by surface acoustic waves and placed in an external flow (Figure 7c).[123] Interestingly, rods moved with their "heads" tilted down toward the substrate, and this was attributed to an interplay between the flow field near a moving rod and its electrostatic interaction with the charged wall. As a result of such tilting, the most energetically favorable configuration of the rod in the presence of an external flow is to align its body in parallel with the flow and move upstream, i.e. rheotaxis.

Although walls are often considered a confinement, accumulating and slowing motors via hydrodynamics and electrokinetics, they can also serve as a critical feature that breaks symmetry and enables propulsion at low Reynolds number (i.e., highly viscous media where inertia becomes negligible). One prominent example is magnetic surface walkers, a type of micromotor that is typically driven by an oscillating magnetic field and rolls on a surface, while their reciprocal motion in the bulk would result in no net displacement. This includes dimers of SiO_2−Ni spheres (Figure 7d),[110] DNA-linked paramagnetic doublets,[124] SiO_2 microspheres coated with $CoFe_2O_4$−$BaTiO_3$ bilayer,[125] microwheels assembled from magnetic colloids,[126] 3D fabricated microstructures coated with magnetic materials,[127] rotating Ni nanowires,[128] a chain of paramagnetic beads,[129] and so on. In these systems, the symmetric rotation of the magnetic particle (or ensemble) produces asymmetric and directional motion, primarily due to an asymmetric fluidic drag that is stronger near the substrate.

Another type of micromotor that relies on the bottom substrate to break symmetry is the recent Quincke roller, which is a dielectric microsphere submerged in organic solvents, exposed to a DC electric field of high strength,

DOI: 10.1021/acsami.8b13103
ACS Appl. Mater. Interfaces XXXX, XXX, XXX−XXX

which rolls on the bottom wall (Figure 7e).[130] Pioneering work from the Bartolo lab have shown that a large number of these Quincke rollers give rise to emergent phenomena such as self-organization into swarms with strong orientational ordering,[131] a vortex,[132] or a prototypical polar fluid.[133] Interesting questions related to active matter can be probed with this micromotor as a model system, an example being how an ordered swarm moves through a disordered system.[131] Although preliminary studies have revealed some interesting features of the interaction between surface walkers or rollers with nearby simple structures (e.g., cracks, steps, and posts), studies with stronger confinements, such as tight channels and porous networks, remain to be seen.

Motors on Liquid–Liquid and Liquid–Gas Interfaces. Another common two-dimensional interface that affects the dynamics of micromotors is liquid–liquid interfaces, typically between water and an organic solvent. Because of the differences in viscosity, chemical solubility, and motor wettability, as well as interfacial forces such as capillarity forces, single particle or collective dynamics of micromotors (especially chemical ones) can be significantly modified. In light of article length limit and to avoid repetition, we direct readers interested in this fascinating and quickly developing research field to a recent review article by the Bishop group.[50]

The third type of two-dimensional interface is liquid–gas interface, or most commonly water–air interface. Compared to liquid–solid and liquid–liquid interfaces, studies of micromotors (except for camphor boats) at water–air interfaces are far less common, and our understanding of this topic remains rather limited. With a large difference in surface tension between water and air, capillary forces and contact lines are certain to be a dominant factor. Indeed, a recent study by Wang et al. revealed a dramatic enhancement of both the persistence length and speeds of 2 μm PS–Pt Janus motors trapped at the interface between air and H_2O_2 aqueous solution (Figures 8a–c).[134] This was attributed to much-decreased rotational diffusion along the interface due to the contract line. Similar micromotors, however, demonstrate very different dynamics on a liquid–liquid interface. Dietrich et al. found experimentally that PS–Pt Janus micromotors could have two different Pt cap orientations when trapped at a water–hexadecane interface and thus showed distinctly different dynamics in H_2O_2[135] and interacted differently with colloidal crystals of PS spheres formed on the interface (Figure 8d).[136]

Moving beyond spherical micromotors, Solovev et al. showed that a rolled-up catalytic micro/nanotube could act as a strider at the air–liquid interface of hydrogen peroxide solution (Figure 8e).[137] They produced oxygen microbubbles at one end of the tip, thus being able to float to the water–air interface by buoyancy. The balance between capillary and drag forces determines assembly and disassembly of the microtubes. Furthermore, by balancing the magnetic attraction and capillary repulsion, Wang et al. presented the dynamic self-assembly of microrafts spinning at an air–water interface.[138] Moreover, there is a large body of research regarding the "camphor boat", a generic name referring to a class of micromotors that float on air–water interfaces and move by Marangoni effect.[139−141] They typically release chemicals of low surface energy in an asymmetric fashion and are thus pulled forward by a surface tension gradient and convective flows. Due to the highly nonlinear nature of their dynamics, oscillation and collective behaviors have been studied in great detail.[142] Finally, we note that although interfacial tension accounts for most of the micromotors moving at the air–water interface, a recent study by Wang et al. demonstrated that the vertical component of a jetting flow from the collapse of oxygen bubbles near a Janus particle can counteract gravity and send the micromotor into a hovering motion underneath the air–water interface.[143]

Rotation Dynamics of Motors. Besides modulating the speeds and collective behaviors of micromotors, a 2D interface offers a unique opportunity to peek into their rotation dynamics. Intentionally or due to fabrication limitations, many, if not most of, micromotors possess some structural asymmetry that propels them into nonlinear trajectories. For example, an arbitrarily fabricated L-shaped particle would move in circles,[120] and so do metal microrods that have imperfectly cylindrical bodies as well as Janus microspheres with imperfect metal coatings.[144] However, the trajectories of many of such asymmetric micromotors often appear Brownian rather than circular, largely because rotational diffusion constantly reorients their bodies, therefore resetting the handedness of their trajectories. When pinned at the air–water interface, on the other hand, such reorientation is significantly suppressed, and Wang et al. thus observed circular trajectories of Pt coated Janus particles at the air–water interface of H_2O_2 solutions.[145] It is not hard to imagine that an air–water interface is not necessary for this "reorientation-pinning" effect to occur. In fact, two previous reports have studied this effect from two different angles. In one study, Takagi et al. noticed that the random but curved trajectories of bimetallic rods undergoing self-electrophoresis near a bottom wall is in fact a result of constant body flipping, without which the curved rods would just move in circles.[146] These curved metallic rods, when powered by ultrasound and compressed into a thin acoustic nodal plane far from any boundaries, indeed showed circular trajectories with constant handedness.[147] In this case, the flipping of the rod bodies is prohibited by the acoustic radiation forces. Overall, these studies reveal an interesting but less noticed aspect of micromotor dynamics, in that the rotational diffusion of asymmetrically shaped particles can be greatly minimized by nearby boundaries.

3.3. 1D Confinements. In most experiments, confinements are in three or two dimensions, while one-dimensional confinements are rarely seen. This is perhaps not beyond imagination because long, thin, and free-standing structures are exceedingly difficult to fabricate. However, in a recent study, Yang et al. offered a creative solution to this problem by magnetically assembling superparamagnetic nanoparticles in a ferrofluid into long chains (Figure 8f).[148] Bubble driven microtubular motors interact with these long chains anisotropically, causing them to move preferably along the chains. This simple, versatile, and real-time technique can be potentially used to regulate the directionality of micromotors.

4. DYNAMICS OF MICROMOTORS MOVING IN THE BULK

To understand the propulsion and interactions of micromotors cruising along boundaries, it is critical to examine their dynamics in the absence of confinement, i.e. swimming in the bulk. This is especially true for those that are powered by self-generated chemical gradients such as bimetallic microrods, Pt coated Janus microspheres, and a variety of self-diffusiophoretic and electrophoretic micromotors. To these micromotors, electroosmosis by the charged bottom and a distortion of both

DOI: 10.1021/acsami.8b13103
ACS Appl. Mater. Interfaces XXXX, XXX, XXX−XXX

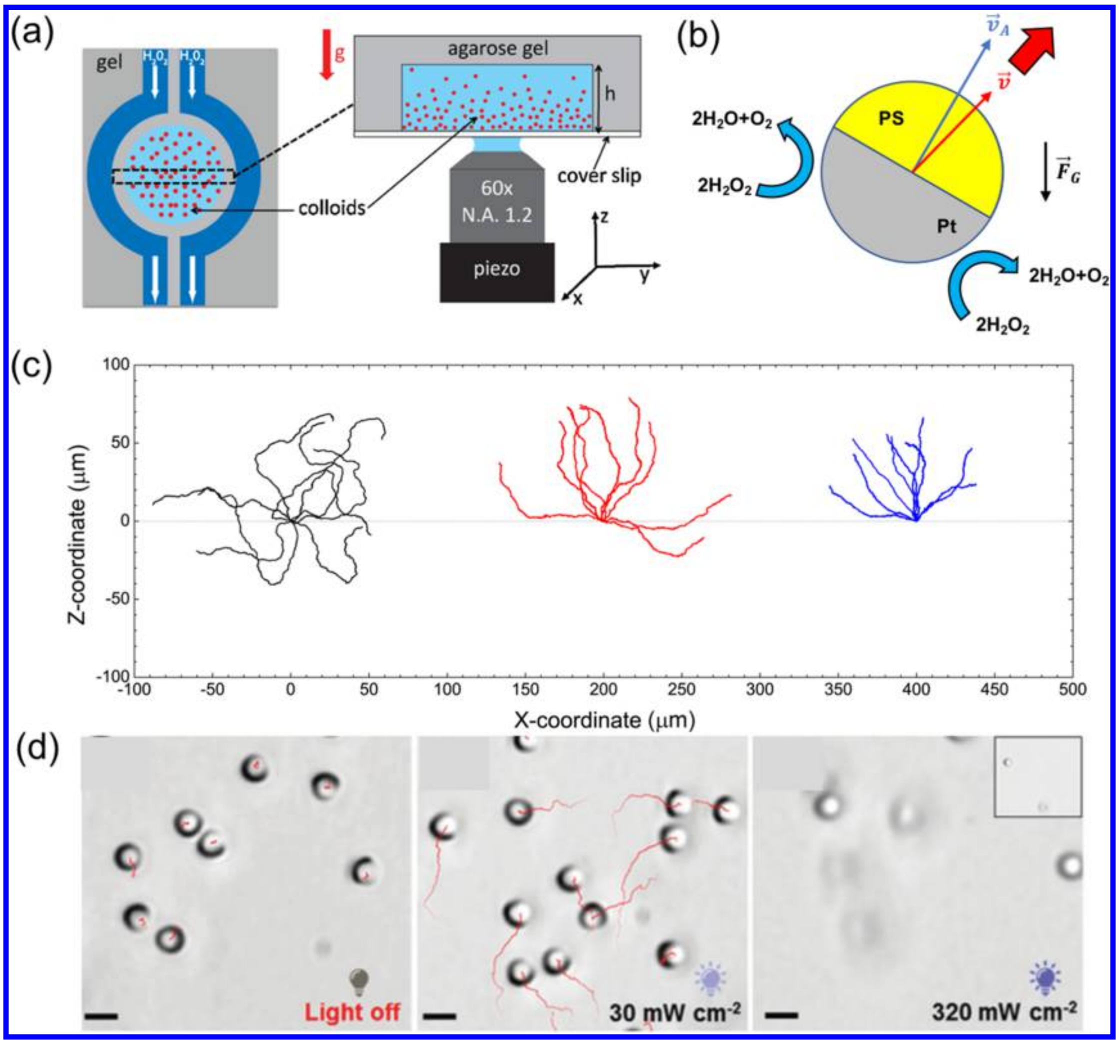

Figure 9. Micromotors moving in the bulk solution. (a) Top view (left) and side view (right) of the experimental setup that studies the sedimentation of Janus micromotors. Reprinted with permission from ref 149. Copyright 2010, American Physical Society. (b) Schematic of the orientation of a bottom-heavy Pt−PS Janus particle and its propulsion upward. Reprinted and adapted with permission from ref 150. Copyright 2017, American Institute of Physics. (c) Trajectories in the *X*−*Z* plane of a Pt coated Janus micromotor of a radius of 0.95 μm (left), 1.55 μm (center), and 2.4 μm (right) moving in 10% H_2O_2. Upward motion becomes more obvious for larger spheres. Reprinted with permission from ref 151. Copyright 2017, American Chemical Society. (d) Optical micrographs showing multiple SiO_2−TiO_2 Janus micromotors moving out of focus when light is applied. Reprinted with permission from ref 152. Copyright 2018, John Wiley and Sons.

the self-generated electric field and chemical gradients can often significantly modify or even dominate motor dynamics and their interactions with nearby active or passive particles. Predicting or understanding experimental observations is therefore complicated. Although arguably much easier to study in theories and simulation, motors moving in the bulk have been experimentally difficult to find, most likely due to the fact that synthetic micromotors are typically heavier than water and readily sediment to the bottom of the experiment chamber, which is commonly glass and induces additional electrokinetic and hydrodynamic effects.

4.1. Recent Studies of Micromotors in the Bulk. A few successful attempts on this topic have mostly involved Janus particles that are (photo)chemically propelled. For example, Palacci et al. studied the steady-state sedimentation distribution of a suspension of PS−Pt Janus particles in H_2O_2 solutions (Figure 9a).[149] Due to an enhanced activity, particles exhibited a significantly different distribution profile from the bottom than that of their passive counterparts, indicating an effective temperature as high as 10^3 K. A separate study performed by Campell et al., on the other hand, showed that the same Janus particles could orient their heavier Pt cap downward and therefore propel away from gravity (antigravitaxis, see Figure 9b).[150] 3D tracking of the trajectories of micromotors swimming in the bulk was achieved by adjusting the *Z*-positions of the stage to keep motors in focus and revealed clear upward motion (Figure 9c). The same group also reported complicated 3D trajectories such as helix when rotation of micromotors was significant.[151] Similar antigravitaxis was also observed with photochemically active Janus motors such as SiO_2−TiO_2[152] (Figure 9d) and poly(methyl methacrylate) (PMMA)−AgCl Janus particles,[68] presumably due to the same density-induced orientation of their active but heavier caps (TiO_2 and AgCl, respectively).

4.2. Techniques Enabling Studies of Micromotors Far from Boundaries. Considering the importance of the study of micromotors in the bulk and the limited success we have had so far that largely relies on motors with heavier but active part tilted downward, new and creative experimental

DOI: 10.1021/acsami.8b13103
ACS Appl. Mater. Interfaces XXXX, XXX, XXX−XXX

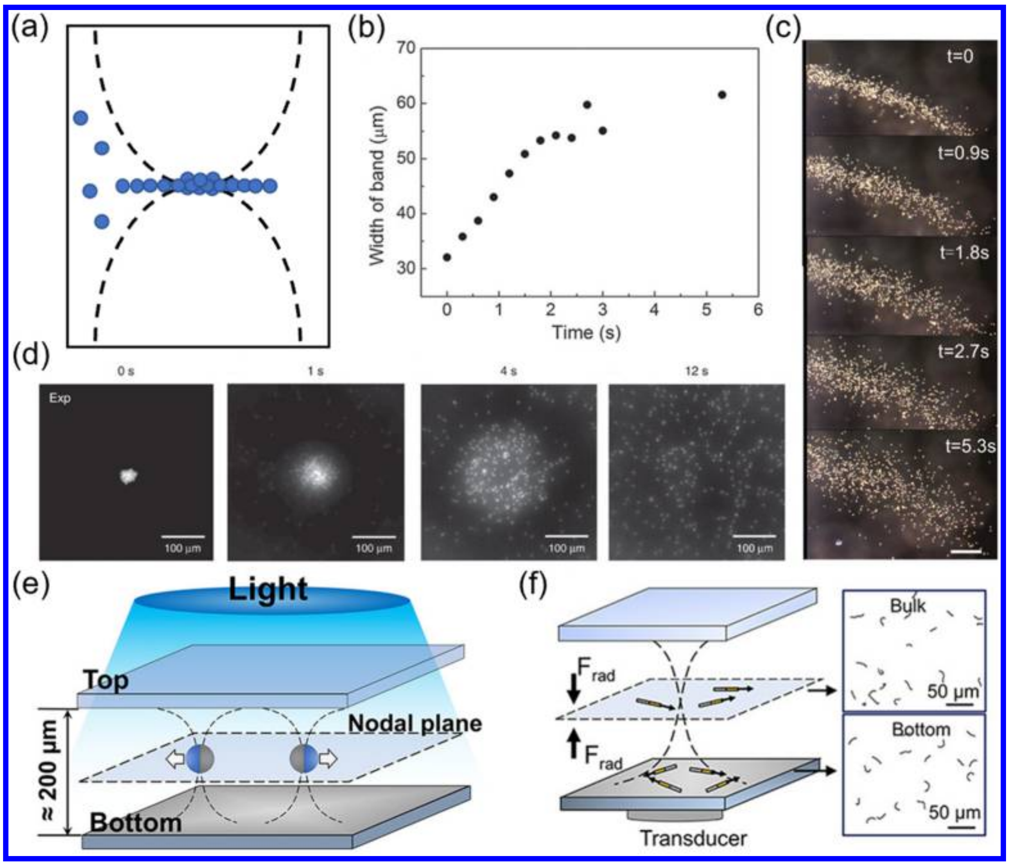

Figure 10. Acoustic trapping as a useful technique for studying micromotors in the bulk. (a) Operating principle of acoustic trapping. Particles are collected at a nodal plane at the center of the experiment chamber by half-wavelength ultrasonic standing waves. Reprinted and adapted with permission from ref 157. Copyright 2012, CCC Republication. (b, c) Expansion of a band of bimetallic micromotors in H_2O_2 that was previously trapped into a nodal line by ultrasound. Reprinted with permission from ref 159. Copyright 2014, CCC Republication. (d) Time-elapsed optical micrographs showing the dispersion of living bacteria from a circular acoustic trap. Reprinted from ref 160, which is licensed under CC BY 4.0. (e) Acoustic levitation is useful for the study of propulsion mechanisms of PMMA−AgCl micromotors under light. Reprinted with permission from ref 68. Copyright 2018, American Chemical Society. (f) Acoustic levitation is used to examine the difference in speed and directionality between bimetallic microrods moving close to a substrate and in the bulk. Reprinted with permission from ref 114. Copyright 2018, American Chemical Society.

techniques that are capable of manipulating micromotors in 3D need to be explored.

Intuitively, one could imagine taking advantage of the fast development of various "tweezer" techniques, such as optical tweezers,[153] magnetic tweezers,[154] and electric tweezers.[155] However, limitations intrinsic to these techniques challenge their usefulness for micromotors. For example, magnetic tweezers require micromotors to include magnetic materials, and complicated 3D arrays of electrodes are possibly needed for electric tweezers. Furthermore, the two hemispheres of a micromotor could polarize differently and therefore experience different dielectrophoretic forces. The impressive improvements of optical tweezers in recent years are promising, yet metal−dielectric Janus particles spontaneously rotate in an optical trap.[156] Manipulation of all-dielectric Janus micromotors (such as SiO_2−TiO_2) by optical tweezers, on the other hand, remains an interesting possibility.

Acoustic traps have recently been demonstrated to be a viable and versatile technique for manipulating micromotors in the bulk. Well-studied for decades, ultrasonic standing waves with wavelengths far larger than the size of micromotors form pressure nodes of well-defined trapping potentials and various configurations, such as a single node, nodal lines, or nodal arrays (Figure 10a).[157,158] Micromotors can then be collected at these nodes and still remain active, and fundamental questions involving active pressure and dispersion of active colloids can also be studied in a controllable fashion, all in the absence of boundary effects. For example, Wang et al. used standing acoustic waves to trap chemically propelled bimetallic micromotors into narrow bands (Figures 10b and c).[159] Motors escaped from the nodal line after the ultrasound was turned off, giving an expanding band of motors that not only changed its distribution over time but also showed a transition in its growth rate that potentially corresponded to the rotational diffusion time of individual motors. In a later and related study, Takatori et al. constructed an acoustic trap where either living bacteria or synthetic micromotors (PS−Pt) were confined (Figure 10d).[160] The distribution of active particles within a 2D harmonic trap was found to be sensitive to the trapping strength, and their "explosion" from the trap after it was turned off revealed a swim pressure that was both sensitive to the confinement size and varied over time after explosion. It is important to note that active particles in both of these studies were moving in the bulk; thus, boundary effects were eliminated.

Acoustic levitation of micromotors can be easily achieved by the propagation of ultrasound of appropriate frequencies in chambers of matching heights. Thus, by lifting micromotors far

DOI: 10.1021/acsami.8b13103
ACS Appl. Mater. Interfaces XXXX, XXX, XXX−XXX

away from any boundaries, the in situ comparison between particle dynamics moving in the bulk and that near a boundary becomes possible. This is extremely useful for elucidating the role of boundary effects on the propulsion and collective behaviors of micromotors. To illustrate its usefulness, we present two examples from our own research lab. In one study, PMMA−AgCl Janus particles were found to move under light illumination.[68] By levitating them 100 μm above the substrate, we confirmed that their motion was qualitatively the same as that near a substrate, suggesting that the electrokinetic effect due to charged bottom substrate that often plagues similar analysis was insignificant (Figure 10e). In a second study, Au−Rh bimetallic microrods moved ~50% faster in the bulk solution than near a charged surface.[113] Acoustic levitation was used to not only reveal this surprising speed difference but also study how functionalizing the surface with polyelectrolytes affected the motor speeds and directionality (Figure 10f).[114]

Although acoustic levitation acts orthogonally on a micromotor to its propulsion mechanism, and therefore is not supposed to modify its activity, we note that ultrasound is known to induce streaming and radiation forces, which could potentially cause motor particles to move and rotate in additional to their original chemical propulsion.[161] We therefore emphasize that such an acoustic propulsion, although useful in a different setting as a biocompatible and powerful energy source for micromotors,[162,163] should be minimized or prevented in the study of motor dynamics when levitated in the bulk. This can be done by either minimizing the ultrasound power, thus minimizing unwanted acoustic propulsion, or by only observing motor dynamics while sedimenting after the ultrasound is turned off (a time window of seconds).

5. SUMMARY AND FUTURE PROSPECTS

Confinements bring interesting questions as well as technical challenges to the fundamental research and applications of micromotors. In this review article, we surveyed tight confinements such as porous networks, tight channels, and narrow grooves, as well as weaker confinements such as the edges of microstructures, interfaces, and chains. Not only do confinements block and redirect micromotor trajectories by physical processes, the speed, directionality, and orientation of confined motors are also profoundly affected by passive and active effects. In addition, many of these effects are sensitive to the propulsion mechanisms of micromotors and the nature of confinements, such as their sizes, shapes, surface chemistry, wettability, viscosity, and so on.

Taken these studies together, it seems more and more clear that boundaries affect micromotors in four distinct ways that may or may not be decoupled from each other. Physically, a wall limits the mass transport of chemical species (reactants and products alike) that are important to a chemical micromotor. How this distortion of chemical concentrations affects micromotors depends heavily on the exact nature of how these chemicals affect micromotors in the first place. Hydrodynamically, a wall is mostly a retarding boundary, slowing nearby micromotors via a no-slip boundary condition that applies to most experiments (unless the wall is intentionally made hydrophobic). Electrostatically, a wall is typically dielectric, and thus "squeezes" any possible electric field that a micromotor generates. To a self-electrophoretic micromotor, this is likely good news because its speed is directly proportional to the field strength. Whether this can be generalized to other systems remains to be studied. A charged wall also electrostatically attracts or repels nearby micromotors, and the sign and magnitude of the charges on their surfaces affects the equilibrium distance between them. Finally, a wall is often electrokinetically responsive, generating electroosmosis in the presence of electric fields. Because the wall often carries a significant amount of charges, the resulting flow can be quite strong, even dominating the flow profile around a micromotor and nearby particles. These four major effects are often closely intertwined, and finding a steady-state solution may require solving complicated partial differential equations in an iterative approach. Computer simulations are therefore extremely useful.

Like the Roman god Janus, where the name Janus particle comes from, we summarize the past and look into the future at the same time. Here, we share our ideas on some potentially interesting directions for future research.

First, we notice that most of the confinements studied so far are inert and unable to respond to micromotors beyond electrokinetics, but it does not have to be that way.[164] Adaptable walls that can respond to forces, chemicals, electric fields, or flows are common in nature, and recent advances in stimuli-responsive materials offer great examples. Responses could manifest in a change in shapes or sizes (e.g., swelling of hydrogels by chemicals or pH), surface charges (e.g., change in ζ-potential), or even electromagnetic properties (e.g., change in magnetic or electric polarization). It is therefore interesting to imagine the presence of a moving motor near a confinement could change the confinement itself, which might further couple back to the motor dynamics through a feedback mechanism and generate interesting nonlinear dynamics such as oscillation or instabilities.

Another way of making confinements more interesting is to break their spatiotemporal symmetry. Although asymmetric microstructures shaped like chevrons,[101] teardrops,[106] and ratchets[107] have been studied, most walls, channels, grooves, or steps are of constant shape. Natural structures, however, are full of wrinkles, bumps, dips, and spikes at the nanoscale and are often functionalized with chemically distinct patches or patterns. Patterns that change over time, on the other hand, are even more rare for artificial confinements. Advances in microfabrication and nonlinear sciences could equip us with powerful tools to fabricate and functionalize the surfaces of various confinements and endow them with time-varying features such as oscillating shapes and electric potentials. Another interesting scenario is confining structures that change dimensions (e.g., a porous network dissociating into free filaments and vice versa), and how the time scale associated with such transition compares to that of micromotor dynamics. The fascinating coupling between dynamic micromotors and spatiotemporally varying confinements remains a fertile ground for future research.

Third, what happens to multiple micromotors in a confinement? The preferred attachment to an interface and its modification of the flow, chemical, and electric field distributions around nearby micromotors could lead to substantially different interparticle interactions and collective behaviors. For example, capillary forces at a liquid−liquid or liquid−air water interfaces are expected to lead to an aggregation of micromotors, while they, via a number of mechanisms, could spontaneously repel. Do we see a stable crystal structure, a phase separation, or unstable dynamic patterns? In a different scenario, one can expect multiple micromotors moving in tight channels to follow each other but

DOI: 10.1021/acsami.8b13103
ACS Appl. Mater. Interfaces XXXX, XXX, XXX−XXX

separated by interparticle repulsions that are common to chemical motors. But do they collectively speed or slow, or do some move faster than others? There is no obvious answer, and it may be sensitive to how the group enters the channel as well as their specific properties.

Fourth, more creative ways are needed to study micromotors in the absence of confinement. Besides using trapping techniques to move micromotors away from bottom walls, there are a few things one could try to more fundamentally address the sedimentation issue, the key reason for which is density mismatch. Therefore, a simple solution is to tune the relative density of the micromotor particle and the liquid medium. For example, instead of coating half of the polymer microsphere with heavy metal such as Pt, which is a common practice for micromotor researchers (see Figure 1b), one could decorate only a small portion of a lightweight polymer sphere with catalytic materials (e.g., MnO_2) in the form of sparsely populated nanoparticles. This micromotor might not be as powerful or efficient as Pt-coated motors, but it could remain suspended and move in 3D for a long time. On the other hand, mixing regular water with deuterated water (aka D_2O or heavy water, density ~1.1 times of H_2O) or glucose gives a significantly heavier medium, to which polymer microspheres such as polystyrene can be perfectly density-matched. Other more exotic ideas include polymer microspheres with air bubbles trapped within to decrease their density, and superhydrophobic particles with surface-trapped air bubbles, and we are only limited by our imaginations.

Finally, we need to apply this knowledge and these fantasies to micromotors and micromachines beyond the commonly studied chemical types. Self-diffusiophoretic and electrophoretic motors produce a complicated interplay among evolving chemical gradients, electric fields, and flow profiles and are therefore very sensitive to external environments. This makes them the ideal candidate (or prime victim, depending on which way you look at this issue) for the study of motor dynamics in confinements. Indeed, most of the literature reviewed here focus on these motors. But there are so many more types of micromotors, with their unique propulsion mechanisms, interaction patterns, and application potentials, but how they operate in confinements remains largely unknown. For example, both thermophoretic micromotors[165] and Janus particles undergoing induced charge electrophoresis (ICEP)[166,167] involve propulsion mechanisms that are relatively better understood and physical process (e.g., heat transfer, electrostatics, and electrokinetic flows) that are sensitive to confinement effects. A systematic study of their dynamics in various degrees of confinement should greatly expand our knowledge on this topic.

Fifteen years after the seminal discovery of the first generations of micromotors,[57,168] this research field is rapidly advancing to more uncharted and complex territories where confinements such as pores, channels, grooves, steps, interfaces, and chains abound. Although we are undoubtedly still in the early days of understanding how micromotors interact with these confinements, the recent surge of interest in this topic has brought about a complicated body of research with many variables and questions but also interesting research opportunities that find clear implications in applications. We are therefore optimistic of the prospect of exploiting confinements for the design of smarter and more powerful micromachinery and structures, such as microbots capable of maneuvering among complex obstacles, microtransporters that shuttle between interfaces and the bulk while carrying out assembling or sensing missions, or even sophisticated microfabricated structures that collect, steer, or pattern cells and microswimmers in any arbitrary fashion, based on simple interaction principles but designed by machine-learning algorithms.

Even though micromotors are often confined, our imaginations are boundless.

AUTHOR INFORMATION

Corresponding Author

*E-mail: weiwangsz@hit.edu.cn or wwang.hitsz@gmail.com.

ORCID

Wei Wang: 0000-0003-4163-3173

Notes

The authors declare no competing financial interest.

ACKNOWLEDGMENTS

We gratefully acknowledge the funding support from the National Natural Science Foundation of China (Grants 11774075 and 11402069), Natural Science Foundation of Guangdong Province (Grant 2017B030306005), and the Science Technology and Innovation Program of Shenzhen (Grant JCYJ20170307150031119).

REFERENCES

(1) Ozin, G. A.; Manners, I.; Fournier-Bidoz, S.; Arsenault, A. Dream Nanomachines. *Adv. Mater.* **2005**, *17* (24), 3011−3018.

(2) Leigh, D. A. Genesis of the nanomachines: The 2016 Nobel Prize in Chemistry. *Angew. Chem., Int. Ed.* **2016**, *55* (47), 14506−14508.

(3) Rapenne, G.; Joachim, C. The First Nanocar Race. *Nat. Rev. Mater.* **2017**, *2*, 17040.

(4) Ariga, K.; Mori, T.; Nakanishi, W. Nano Trek Beyond: Driving Nanocars/Molecular Machines at Interfaces. *Chem. - Asian J.* **2018**, *13* (10), 1266−1278.

(5) Wang, J. *Nanomachines: Fundamentals and Applications*; Wiley-VCH: Weinheim, Germany, 2013.

(6) Mallouk, T. E.; Sen, A. Powering Nanorobots. *Sci. Am.* **2009**, *300* (5), 72−77.

(7) Kim, K.; Guo, J.; Xu, X.; Fan, D. Recent Progress on Man-Made Inorganic Nanomachines. *Small* **2015**, *11* (33), 4037−4057.

(8) Wang, W.; Duan, W.; Ahmed, S.; Mallouk, T. E.; Sen, A. Small Power: Autonomous Nano-and Micromotors Propelled by Self-Generated Gradients. *Nano Today* **2013**, *8* (5), 531−554.

(9) Sengupta, S.; Ibele, M. E.; Sen, A. Fantastic Voyage: Designing Self-Powered Nanorobots. *Angew. Chem., Int. Ed.* **2012**, *51* (34), 8434−8445.

(10) Sanchez, S.; Pumera, M. Nanorobots: The Ultimate Wireless Self-Propelled Sensing and Actuating Devices. *Chem. - Asian J.* **2009**, *4* (9), 1402−1410.

(11) Ebbens, S. J.; Howse, J. R. In Pursuit of Propulsion at the Nanoscale. *Soft Matter* **2010**, *6* (4), 726−738.

(12) Feynman, R. P. There's Plenty of Room at the Bottom: An Invitation to Enter a New Field of Physics. In *Handbook of Nanoscience, Engineering, and Technology*, 3rd ed.; CRC Press: 2012; pp 26−35.

(13) Hu, C.; Pané, S.; Nelson, B. J. Soft Micro-and Nanorobotics. *Annu. Rev. Contr. Robot. Auto. Syst.* **2018**, *1*, 53−75.

(14) Medina-Sánchez, M.; Magdanz, V.; Guix, M.; Fomin, V. M.; Schmidt, O. G. Swimming Microrobots: Soft, Reconfigurable, and Smart. *Adv. Funct. Mater.* **2018**, *28*, 1707228.

(15) Cho, S. K. Mini and Micro Propulsion for Medical Swimmers. *Micromachines* **2014**, *5* (1), 97−113.

(16) Nelson, B. J.; Kaliakatsos, I. K.; Abbott, J. J. Microrobots for Minimally Invasive Medicine. *Annu. Rev. Biomed. Eng.* **2010**, *12*, 55−85.
(17) Li, J.; de Ávila, B. E.-F.; Gao, W.; Zhang, L.; Wang, J. Micro/Nanorobots for Biomedicine: Delivery, Surgery, Sensing, and Detoxification. *Sci. Robot.* **2017**, *2* (4), eaam6431.
(18) Parmar, J.; Vilela, D.; Villa, K.; Wang, J.; Sanchez, S. Micro-and Nanomotors as Active Environmental Microcleaners and Sensors. *J. Am. Chem. Soc.* **2018**, *140* (30), 9317−9331.
(19) Singh, V. V.; Wang, J. Nano/Micromotors for Security/Defense Applications. A Review. *Nanoscale* **2015**, *7* (46), 19377−19389.
(20) Mallory, S. A.; Valeriani, C.; Cacciuto, A. An Active Approach to Colloidal Self-Assembly. *Annu. Rev. Phys. Chem.* **2018**, *69*, 59−79.
(21) Hänggi, P.; Marchesoni, F. Artificial Brownian Motors: Controlling Transport on the Nanoscale. *Rev. Mod. Phys.* **2009**, *81* (1), 387.
(22) Burada, P. S.; Hänggi, P.; Marchesoni, F.; Schmid, G.; Talkner, P. Diffusion in Confined Geometries. *ChemPhysChem* **2009**, *10* (1), 45−54.
(23) Yang, X.; Liu, C.; Li, Y.; Marchesoni, F.; Hänggi, P.; Zhang, H. Hydrodynamic and Entropic Effects on Colloidal Diffusion in Corrugated Channels. *Proc. Natl. Acad. Sci. U. S. A.* **2017**, *114* (36), 9564−9569.
(24) Burada, P.; Schmid, G.; Talkner, P.; Hänggi, P.; Reguera, D.; Rubí, J. M. Entropic Particle Transport in Periodic Channels. *BioSystems* **2008**, *93* (1−2), 16−22.
(25) Reguera, D.; Schmid, G.; Burada, P. S.; Rubi, J.; Reimann, P.; Hänggi, P. Entropic Transport: Kinetics, Scaling, and Control Mechanisms. *Phys. Rev. Lett.* **2006**, *96* (13), 130603.
(26) Oster, G. Brownian Ratchets: Darwin's Motors. *Nature* **2002**, *417* (6884), 25.
(27) Peskin, C. S.; Odell, G. M.; Oster, G. F. Cellular Motions and Thermal Fluctuations: the Brownian Ratchet. *Biophys. J.* **1993**, *65* (1), 316−324.
(28) Kettner, C.; Reimann, P.; Hänggi, P.; Müller, F. Drift Ratchet. *Phys. Rev. E: Stat. Phys., Plasmas, Fluids, Relat. Interdiscip. Top.* **2000**, *61* (1), 312.
(29) Müller, F.; Birner, A.; Schilling, J.; Gösele, U.; Kettner, C.; Hänggi, P. Membranes for Micropumps from Macroporous Silicon. *Phys. Status Solidi (a)* **2000**, *182* (1), 585−590.
(30) Matthias, S.; Müller, F. Asymmetric Pores in a Silicon Membrane Acting as Massively Parallel Brownian Ratchets. *Nature* **2003**, *424* (6944), 53.
(31) Jana, S.; Um, S. H.; Jung, S. Paramecium Swimming in Capillary Tube. *Phys. Fluids* **2012**, *24* (4), No. 041901.
(32) Männik, J.; Driessen, R.; Galajda, P.; Keymer, J. E.; Dekker, C. Bacterial Growth and Motility in Sub-Micron Constrictions. *Proc. Natl. Acad. Sci. U. S. A.* **2009**, *106* (35), 14861−14866.
(33) Zhu, L.; Lauga, E.; Brandt, L. Low-Reynolds-Number Swimming in a Capillary Tube. *J. Fluid Mech.* **2013**, *726*, 285−311.
(34) Acemoglu, A.; Yesilyurt, S. Effects of Geometric Parameters on Swimming of Micro Organisms with Single Helical Flagellum in Circular Channels. *Biophys. J.* **2014**, *106* (7), 1537−1547.
(35) Wu, H.; Thiébaud, M.; Hu, W.-F.; Farutin, A.; Rafaï, S.; Lai, M.-C.; Peyla, P.; Misbah, C. Amoeboid Motion in Confined Geometry. *Phys. Rev. E* **2015**, *92* (5), e050701.
(36) Felderhof, B. Swimming at low Reynolds Number of a Cylindrical Body in a Circular Tube. *Phys. Fluids* **2010**, *22* (11), 113604.
(37) Liu, B.; Breuer, K. S.; Powers, T. R. Propulsion by a Helical Flagellum in a Capillary Tube. *Phys. Fluids* **2014**, *26* (1), No. 011701.
(38) Ledesma-Aguilar, R.; Yeomans, J. M. Enhanced Motility of a Microswimmer in Rigid and Elastic Confinement. *Phys. Rev. Lett.* **2013**, *111* (13), 138101.
(39) Schamel, D.; Mark, A. G.; Gibbs, J. G.; Miksch, C.; Morozov, K. I.; Leshansky, A. M.; Fischer, P. Nanopropellers and Their Actuation in Complex Viscoelastic Media. *ACS Nano* **2014**, *8* (9), 8794−8801.
(40) Cheng, R.; Huang, W.; Huang, L.; Yang, B.; Mao, L.; Jin, K.; ZhuGe, Q.; Zhao, Y. Acceleration of Tissue Plasminogen Activator-Mediated Thrombolysis by Magnetically Powered Nanomotors. *ACS Nano* **2014**, *8* (8), 7746−7754.
(41) Yan, X.; Zhou, Q.; Vincent, M.; Deng, Y.; Yu, J.; Xu, J.; Xu, T.; Tang, T.; Bian, L.; Wang, Y.-X. J. Multifunctional Biohybrid Magnetite Microrobots for Imaging-Guided Therapy. *Sci. Robot* **2017**, *2* (12), eaaq1155.
(42) Shao, J.; Abdelghani, M.; Shen, G.; Cao, S.; Williams, D. S.; Van Hest, J. C. Erythrocyte Membrane Modified Janus Polymeric Motors for Thrombus Therapy. *ACS Nano* **2018**, *12* (5), 4877−4885.
(43) Wu, Z.; Li, T.; Li, J.; Gao, W.; Xu, T.; Christianson, C.; Gao, W.; Galarnyk, M.; He, Q.; Zhang, L. Turning Erythrocytes into Functional Micromotors. *ACS Nano* **2014**, *8* (12), 12041−12048.
(44) Magdanz, V.; Sanchez, S.; Schmidt, O. G. Development of a Sperm-Flagella Driven Micro-Bio-Robot. *Adv. Mater.* **2013**, *25* (45), 6581−6588.
(45) Gao, W.; Dong, R.; Thamphiwatana, S.; Li, J.; Gao, W.; Zhang, L.; Wang, J. Artificial Micromotors in the Mouse's Stomach: A Step toward in Vivo Use of Synthetic Motors. *ACS Nano* **2015**, *9* (1), 117−123.
(46) Burdick, J.; Laocharoensuk, R.; Wheat, P. M.; Posner, J. D.; Wang, J. Synthetic Nanomotors in Microchannel Networks: Directional Microchip Motion and Controlled Manipulation of Cargo. *J. Am. Chem. Soc.* **2008**, *130* (26), 8164−8165.
(47) Baraban, L.; Makarov, D.; Streubel, R.; Monch, I.; Grimm, D.; Sanchez, S.; Schmidt, O. G. Catalytic Janus Motors on Microfluidic Chip: Deterministic Motion for Targeted Cargo Delivery. *ACS Nano* **2012**, *6* (4), 3383−3389.
(48) Zhou, C.; Zhang, H.; Li, Z.; Wang, W. Chemistry Pumps: A Review of Chemically Powered Micropumps. *Lab Chip* **2016**, *16* (10), 1797−1811.
(49) Kherzi, B.; Pumera, M. Self-propelled Autonomous Nanomotors Meet Microfluidics. *Nanoscale* **2016**, *8* (40), 17415−17421.
(50) Fei, W.; Gu, Y.; Bishop, K. J. Active Colloidal Particles at Fluid-Fluid Interfaces. *Curr. Opin. Colloid Interface Sci.* **2017**, *32*, 57−68.
(51) Patteson, A. E.; Gopinath, A.; Arratia, P. E. Active Colloids in Complex Fluids. *Curr. Opin. Colloid Interface Sci.* **2016**, *21*, 86−96.
(52) Bechinger, C.; Di Leonardo, R.; Löwen, H.; Reichhardt, C.; Volpe, G.; Volpe, G. Active Particles in Complex and Crowded Environments. *Rev. Mod. Phys.* **2016**, *88* (4), No. 045006.
(53) Katuri, J.; Seo, K.; Kim, D.; Sanchez, S. Artificial Micro-Swimmers in Simulated Natural Environments. *Lab Chip* **2016**, *16* (7), 1101−1105.
(54) Jurado-Sanchez, B.; Pacheco, M.; Maria-Hormigos, R.; Escarpa, A. Perspectives on Janus Micromotors: Materials and Applications. *Applied Materials Today* **2017**, *9*, 407−418.
(55) Pourrahimi, A. M.; Pumera, M. Multifunctional and Self-propelled Spherical Janus Nano/Micromotors: Recent Advances. *Nanoscale* **2018**, *10*, 16398−16415.
(56) Archer, R. J.; Parnell, A. J.; Campbell, A. I.; Howse, J. R.; Ebbens, S. J. A Pickering Emulsion Route to Swimming Active Janus Colloids. *Advanced Science* **2018**, *5* (2), 1700528.
(57) Paxton, W. F.; Kistler, K. C.; Olmeda, C. C.; Sen, A.; St. Angelo, S. K.; Cao, Y.; Mallouk, T. E.; Lammert, P. E.; Crespi, V. H. Catalytic Nanomotors: Autonomous Movement of Striped Nanorods. *J. Am. Chem. Soc.* **2004**, *126* (41), 13424−13431.
(58) Wang, Y.; Hernandez, R. M.; Bartlett, D. J.; Bingham, J. M.; Kline, T. R.; Sen, A.; Mallouk, T. E. Bipolar Electrochemical Mechanism for the Propulsion of Catalytic Nanomotors in Hydrogen Peroxide Solutions. *Langmuir* **2006**, *22* (25), 10451−10456.
(59) Wong, F.; Sen, A. Progress toward Light-Harvesting Self-Electrophoretic Motors: Highly Efficient Bimetallic Nanomotors and Micropumps in Halogen Media. *ACS Nano* **2016**, *10* (7), 7172−7179.
(60) Liu, R.; Sen, A. Autonomous Nanomotor Based on Copper−Platinum Segmented Nanobattery. *J. Am. Chem. Soc.* **2011**, *133* (50), 20064−20067.
(61) Dong, R.; Zhang, Q.; Gao, W.; Pei, A.; Ren, B. Highly Efficient Light-Driven TiO_2−Au Janus Micromotors. *ACS Nano* **2016**, *10* (1), 839−844.

(62) Zhou, D.; Ren, L.; Li, Y. C.; Xu, P.; Gao, Y.; Zhang, G.; Wang, W.; Mallouk, T. E.; Li, L. Visible Light-Driven, Magnetically Steerable Gold/Iron Oxide Nanomotors. *Chem. Commun.* **2017**, *53* (83), 11465−11468.

(63) Kong, L.; Mayorga-Martinez, C. C.; Guan, J.; Pumera, M. Fuel-Free Light-Powered TiO2/Pt Janus Micromotors for Enhanced Nitroaromatic Explosives Degradation. *ACS Appl. Mater. Interfaces* **2018**, *10* (26), 22427−22434.

(64) Velegol, D.; Garg, A.; Guha, R.; Kar, A.; Kumar, M. Origins of Concentration Gradients for Diffusiophoresis. *Soft Matter* **2016**, *12* (21), 4686−4703.

(65) Popescu, M. N.; Uspal, W. E.; Dietrich, S. Self-Diffusiophoresis of Chemically Active Colloids. *Eur. Phys. J.: Spec. Top.* **2016**, *225* (11−12), 2189−2206.

(66) Moran, J. L.; Posner, J. D. Phoretic Self-Propulsion. *Annu. Rev. Fluid Mech.* **2017**, *49*, 511−540.

(67) Anderson, J. L. Colloid Transport by Interfacial Forces. *Annu. Rev. Fluid Mech.* **1989**, *21* (1), 61−99.

(68) Zhou, C.; Zhang, H.; Tang, J.; Wang, W. Photochemically Powered AgCl Janus Micromotors as a Model System to Understand Ionic Self-Diffusiophoresis. *Langmuir* **2018**, *34* (10), 3289−3295.

(69) Ebbens, S. J.; Howse, J. R. Direct Observation of the Direction of Motion for Spherical Catalytic Swimmers. *Langmuir* **2011**, *27* (20), 12293−12296.

(70) Howse, J. R.; Jones, R. A.; Ryan, A. J.; Gough, T.; Vafabakhsh, R.; Golestanian, R. Self-Motile Colloidal Particles: From Directed Propulsion to Random Walk. *Phys. Rev. Lett.* **2007**, *99* (4), No. 048102.

(71) Hong, Y.; Diaz, M.; Córdova-Figueroa, U. M.; Sen, A. Light-Driven Titanium-Dioxide-Based Reversible Microfireworks and Micromotor/Micropump Systems. *Adv. Funct. Mater.* **2010**, *20* (10), 1568−1576.

(72) Chen, C.; Mou, F.; Xu, L.; Wang, S.; Guan, J.; Feng, Z.; Wang, Q.; Kong, L.; Li, W.; Wang, J. Light-Steered Isotropic Semiconductor Micromotors. *Adv. Mater.* **2017**, *29* (3), 1603374.

(73) Singh, D. P.; Choudhury, U.; Fischer, P.; Mark, A. G. Non-Equilibrium Assembly of Light-Activated Colloidal Mixtures. *Adv. Mater.* **2017**, *29* (32), 1701328.

(74) Ibele, M.; Mallouk, T. E.; Sen, A. Schooling Behavior of Light-Powered Autonomous Micromotors in Water. *Angew. Chem.* **2009**, *121* (18), 3358−3362.

(75) Ma, X.; Hortelão, A. C.; Patiño, T.; Sánchez, S. Enzyme Catalysis to Power Micro/Nanomachines. *ACS Nano* **2016**, *10* (10), 9111−9122.

(76) Dey, K. K.; Zhao, X.; Tansi, B. M.; Méndez-Ortiz, W. J.; Córdova-Figueroa, U. M.; Golestanian, R.; Sen, A. Micromotors Powered by Enzyme Catalysis. *Nano Lett.* **2015**, *15* (12), 8311−8315.

(77) Sengupta, S.; Patra, D.; Ortiz-Rivera, I.; Agrawal, A.; Shklyaev, S.; Dey, K. K.; Córdova-Figueroa, U.; Mallouk, T. E.; Sen, A. Self-Powered Enzyme Micropumps. *Nat. Chem.* **2014**, *6* (5), 415.

(78) Ebbens, S.; Gregory, D.; Dunderdale, G.; Howse, J.; Ibrahim, Y.; Liverpool, T.; Golestanian, R. Electrokinetic Effects in Catalytic Platinum-Insulator Janus Swimmers. *Europhys. Lett.* **2014**, *106* (5), 58003.

(79) Brown, A. T.; Poon, W. C.; Holm, C.; de Graaf, J. Ionic Screening and Dissociation are Crucial for Understanding Chemical Self-Propulsion in Polar Solvents. *Soft Matter* **2017**, *13* (6), 1200−1222.

(80) Li, J.; Rozen, I.; Wang, J. Rocket Science at the Nanoscale. *ACS Nano* **2016**, *10* (6), 5619−5634.

(81) Xu, T.; Gao, W.; Xu, L. P.; Zhang, X.; Wang, S. Fuel-Free Synthetic Micro-/Nanomachines. *Adv. Mater.* **2017**, *29* (9), 1603250.

(82) Chen, X. Z.; Jang, B.; Ahmed, D.; Hu, C.; De Marco, C.; Hoop, M.; Mushtaq, F.; Nelson, B. J.; Pané, S. Small-Scale Machines Driven by External Power Sources. *Adv. Mater.* **2018**, *30* (15), 1705061.

(83) Popescu, M. N.; Dietrich, S.; Oshanin, G. Confinement Effects on Diffusiophoretic Self-Propellers. *J. Chem. Phys.* **2009**, *130* (19), 194702.

(84) Wang, W.; Li, S.; Mair, L.; Ahmed, S.; Huang, T. J.; Mallouk, T. E. Acoustic Propulsion of Nanorod Motors inside Living Cells. *Angew. Chem., Int. Ed.* **2014**, *53* (12), 3201−3204.

(85) Volpe, G.; Buttinoni, I.; Vogt, D.; Kümmerer, H.-J.; Bechinger, C. Microswimmers in Patterned Environments. *Soft Matter* **2011**, *7* (19), 8810−8815.

(86) Spagnolie, S. E.; Liu, B.; Powers, T. R. Locomotion of Helical Bodies in Viscoelastic Fluids: Enhanced Swimming at Large Helical Amplitudes. *Phys. Rev. Lett.* **2013**, *111* (6), No. 068101.

(87) Leshansky, A. Enhanced Low-Reynolds-Number Propulsion in Heterogeneous Viscous Environments. *Phys. Rev. E* **2009**, *80* (5), No. 051911.

(88) Fu, H. C.; Shenoy, V. B.; Powers, T. R. Low-Reynolds-Number Swimming in Gels. *Europhys. Lett.* **2010**, *91* (2), 24002.

(89) Walker, D.; Käsdorf, B. T.; Jeong, H.-H.; Lieleg, O.; Fischer, P. Enzymatically Active Biomimetic Micropropellers for the Penetration of Mucin Gels. *Sci. Adv.* **2015**, *1* (11), No. e1500501.

(90) Gomez-Solano, J. R.; Blokhuis, A.; Bechinger, C. Dynamics of Self-Propelled Janus Particles in Viscoelastic Fluids. *Phys. Rev. Lett.* **2016**, *116* (13), 138301.

(91) Ahmed, D.; Lu, M.; Nourhani, A.; Lammert, P. E.; Stratton, Z.; Muddana, H. S.; Crespi, V. H.; Huang, T. J. Selectively Manipulable Acoustic-Powered Microswimmers. *Sci. Rep.* **2015**, *5*, 9744.

(92) Han, K.; Shields, C. W.; Diwakar, N. M.; Bharti, B.; López, G. P.; Velev, O. D. Sequence-Encoded Colloidal Origami and Microbot Assemblies from Patchy Magnetic Cubes. *Sci. Adv.* **2017**, *3* (8), No. e1701108.

(93) Yang, F.; Qian, S.; Zhao, Y.; Qiao, R. Self-Diffusiophoresis of Janus Catalytic Micromotors in Confined Geometries. *Langmuir* **2016**, *32* (22), 5580−5592.

(94) Liu, C.; Zhou, C.; Wang, W.; Zhang, H. Bimetallic Microswimmers Speed Up in Confining Channels. *Phys. Rev. Lett.* **2016**, *117* (19), 198001.

(95) Yu, H.; Kopach, A.; Misko, V. R.; Vasylenko, A. A.; Makarov, D.; Marchesoni, F.; Nori, F.; Baraban, L.; Cuniberti, G. Confined Catalytic Janus Swimmers in a Crowded Channel: Geometry-Driven Rectification Transients and Directional Locking. *Small* **2016**, *12* (42), 5882−5890.

(96) Wensink, H.; Löwen, H. Aggregation of Self-Propelled Colloidal Rods near Confining Walls. *Phys. Rev. E* **2008**, *78* (3), No. 031409.

(97) Palacci, J.; Sacanna, S.; Vatchinsky, A.; Chaikin, P. M.; Pine, D. J. Photoactivated Colloidal Dockers for Cargo Transportation. *J. Am. Chem. Soc.* **2013**, *135* (43), 15978−15981.

(98) Das, S.; Garg, A.; Campbell, A. I.; Howse, J.; Sen, A.; Velegol, D.; Golestanian, R.; Ebbens, S. J. Boundaries Can Steer Active Janus Spheres. *Nat. Commun.* **2015**, *6*, 8999.

(99) Simmchen, J.; Katuri, J.; Uspal, W. E.; Popescu, M. N.; Tasinkevych, M.; Sánchez, S. Topographical Pathways Guide Chemical Microswimmers. *Nat. Commun.* **2016**, *7*, 10598.

(100) Kaiser, A.; Popowa, K.; Wensink, H.; Löwen, H. Capturing Self-Propelled Particles in a Moving Microwedge. *Phys. Rev. E* **2013**, *88* (2), No. 022311.

(101) Restrepo-Pérez, L.; Soler, L.; Martínez-Cisneros, C. S.; Sánchez, S.; Schmidt, O. G. Trapping Self-Propelled Micromotors with Microfabricated Chevron and Heart-Shaped Chips. *Lab Chip* **2014**, *14* (9), 1515−1518.

(102) Parisi, D. R.; Hidalgo, R. C.; Zuriguel, I. Active Particles with Desired Orientation Flowing through a Bottleneck. *Sci. Rep.* **2018**, *8* (1), 9133.

(103) Takagi, D.; Palacci, J.; Braunschweig, A. B.; Shelley, M. J.; Zhang, J. Hydrodynamic Capture of Microswimmers into Sphere-Bound Orbits. *Soft Matter* **2014**, *10* (11), 1784−1789.

(104) Brown, A. T.; Vladescu, I. D.; Dawson, A.; Vissers, T.; Schwarz-Linek, J.; Lintuvuori, J. S.; Poon, W. C. Swimming in a Crystal. *Soft Matter* **2016**, *12* (1), 131−140.

(105) Chen, Y.-F.; Xiao, S.; Chen, H.-Y.; Sheng, Y.-J.; Tsao, H.-K. Enhancing Rectification of a Nano-Swimmer System by Multi-Layered Asymmetric Barriers. *Nanoscale* **2015**, *7* (39), 16451−16459.

DOI: 10.1021/acsami.8b13103
ACS Appl. Mater. Interfaces XXXX, XXX, XXX−XXX

(106) Wykes, M. S. D.; Zhong, X.; Tong, J.; Adachi, T.; Liu, Y.; Ristroph, L.; Ward, M. D.; Shelley, M. J.; Zhang, J. Guiding Microscale Swimmers Using Teardrop-Shaped Posts. *Soft Matter* **2017**, *13* (27), 4681−4688.
(107) Katuri, J.; Caballero, D.; Voituriez, R.; Samitier, J.; Sanchez, S. Directed Flow of Micromotors through Alignment Interactions with Micropatterned Ratchets. *ACS Nano* **2018**, *12* (7), 7282−7291.
(108) Mijalkov, M.; Volpe, G. Sorting of Chiral Microswimmers. *Soft Matter* **2013**, *9* (28), 6376−6381.
(109) Choudhury, U.; Straube, A. V.; Fischer, P.; Gibbs, J. G.; Höfling, F. Active Colloidal Propulsion over a Crystalline Surface. *New J. Phys.* **2017**, *19* (12), 125010.
(110) Li, T.; Zhang, A.; Shao, G.; Wei, M.; Guo, B.; Zhang, G.; Li, L.; Wang, W. Janus Microdimer Surface Walkers Propelled by Oscillating Magnetic Fields. *Adv. Funct. Mater.* **2018**, *28*, 1706066.
(111) Shen, Z.; Würger, A.; Lintuvuori, J. S. Hydrodynamic Interaction of a Self-Propelling Particle with a Wall. *Eur. Phys. J. E: Soft Matter Biol. Phys.* **2018**, *41* (3), 39.
(112) Chiang, T.-Y.; Velegol, D. Localized Electroosmosis (LEO) Induced by Spherical Colloidal Motors. *Langmuir* **2014**, *30* (10), 2600−2607.
(113) Wang, W.; Chiang, T.-Y.; Velegol, D.; Mallouk, T. E. Understanding the Efficiency of Autonomous Nano-and Microscale Motors. *J. Am. Chem. Soc.* **2013**, *135* (28), 10557−10565.
(114) Wei, M.; Zhou, C.; Tang, J.; Wang, W. Catalytic Micromotors Moving Near Polyelectrolyte-Modified Substrates: The Roles of Surface Charges, Morphology, and Released Ions. *ACS Appl. Mater. Interfaces* **2018**, *10* (3), 2249−2252.
(115) Nicholls, D.; DeVerse, A.; Esplin, R. S.; Castañeda, J.; Loyd, Y.; Nair, R.; Voinescu, R.; Zhou, C.; Wang, W.; Gibbs, J. G. Shape-Dependent Motion of Structured Photoactive Microswimmers. *ACS Appl. Mater. Interfaces* **2018**, *10* (21), 18050−18056.
(116) Yariv, E. Wall-Induced Self-Diffusiophoresis of Active Isotropic Colloids. *Phys. Rev. Fluids* **2016**, *1* (3), No. 032101.
(117) Palacci, J.; Sacanna, S.; Kim, S.-H.; Yi, G.-R.; Pine, D.; Chaikin, P. Light-Activated Self-Propelled Colloids. *Philos. Trans. R. Soc., A* **2014**, *372* (2029), 20130372.
(118) Uspal, W.; Popescu, M. N.; Dietrich, S.; Tasinkevych, M. Self-Propulsion of a Catalytically Active Particle near a Planar Wall: From Reflection to Sliding and Hovering. *Soft Matter* **2015**, *11* (3), 434−438.
(119) Mozaffari, A.; Sharifi-Mood, N.; Koplik, J.; Maldarelli, C. Self-Diffusiophoretic Colloidal Propulsion near a Solid Boundary. *Phys. Fluids* **2016**, *28* (5), No. 053107.
(120) Kümmel, F.; ten Hagen, B.; Wittkowski, R.; Buttinoni, I.; Eichhorn, R.; Volpe, G.; Löwen, H.; Bechinger, C. Circular Motion of Asymmetric Self-Propelling Particles. *Phys. Rev. Lett.* **2013**, *110* (19), 198302.
(121) Ibrahim, Y.; Liverpool, T. B. The Dynamics of a Self-Phoretic Janus Swimmer near a Wall. *Europhys. Lett.* **2015**, *111* (4), 48008.
(122) Volpe, G.; Gigan, S.; Volpe, G. Simulation of the Active Brownian Motion of a Microswimmer. *Am. J. Phys.* **2014**, *82* (7), 659−664.
(123) Ren, L.; Zhou, D.; Mao, Z.; Xu, P.; Huang, T. J.; Mallouk, T. E. Rheotaxis of Bimetallic Micromotors Driven by Chemical−Acoustic Hybrid Power. *ACS Nano* **2017**, *11* (10), 10591−10598.
(124) Tierno, P.; Golestanian, R.; Pagonabarraga, I.; Sagués, F. Controlled Swimming in Confined Fluids of Magnetically Actuated Colloidal Rotors. *Phys. Rev. Lett.* **2008**, *101* (21), 218304.
(125) Chen, X.-Z.; Shamsudhin, N.; Hoop, M.; Pieters, R.; Siringil, E.; Sakar, M. S.; Nelson, B. J.; Pané, S. Magnetoelectric Micromachines with Wirelessly Controlled Navigation and Functionality. *Mater. Horiz.* **2016**, *3* (2), 113−118.
(126) Tasci, T.; Herson, P.; Neeves, K.; Marr, D. Surface-Enabled Propulsion and Control of Colloidal Microwheels. *Nat. Commun.* **2016**, *7*, 10225.
(127) Kim, S.; Qiu, F.; Kim, S.; Ghanbari, A.; Moon, C.; Zhang, L.; Nelson, B. J.; Choi, H. Fabrication and Characterization of Magnetic Microrobots for Three-Dimensional Cell Culture and Targeted Transportation. *Adv. Mater.* **2013**, *25* (41), 5863−5868.
(128) Petit, T.; Zhang, L.; Peyer, K. E.; Kratochvil, B. E.; Nelson, B. J. Selective Trapping and Manipulation of Microscale Objects Using Mobile Microvortices. *Nano Lett.* **2012**, *12* (1), 156−160.
(129) Sing, C. E.; Schmid, L.; Schneider, M. F.; Franke, T.; Alexander-Katz, A. Controlled Surface-Induced Flows From the Motion of Self-Assembled Colloidal Walkers. *Proc. Natl. Acad. Sci. U. S. A.* **2010**, *107* (2), 535−540.
(130) Bricard, A.; Caussin, J.-B.; Desreumaux, N.; Dauchot, O.; Bartolo, D. Emergence of Macroscopic Directed Motion in Populations of Motile Colloids. *Nature* **2013**, *503* (7474), 95.
(131) Morin, A.; Desreumaux, N.; Caussin, J.-B.; Bartolo, D. Distortion and Destruction of Colloidal Flocks in Disordered Environments. *Nat. Phys.* **2016**, *13* (1), 63.
(132) Bricard, A.; Caussin, J.-B.; Das, D.; Savoie, C.; Chikkadi, V.; Shitara, K.; Chepizhko, O.; Peruani, F.; Saintillan, D.; Bartolo, D. Emergent Vortices in Populations of Colloidal Rollers. *Nat. Commun.* **2015**, *6*, 7470.
(133) Geyer, D.; Morin, A.; Bartolo, D. Sounds and Hydrodynamics of Polar Active Fluids. *Nat. Mater.* **2018**, *17*, 789−793.
(134) Wang, X.; In, M.; Blanc, C.; Nobili, M.; Stocco, A. Enhanced Active Motion of Janus Colloids at the Water Surface. *Soft Matter* **2015**, *11* (37), 7376−7384.
(135) Dietrich, K.; Renggli, D.; Zanini, M.; Volpe, G.; Buttinoni, I.; Isa, L. Two-Dimensional Nature of the Active Brownian Motion of Catalytic Microswimmers at Solid and Liquid Interfaces. *New J. Phys.* **2017**, *19* (6), No. 065008.
(136) Dietrich, K.; Volpe, G.; Sulaiman, M. N.; Renggli, D.; Buttinoni, I.; Isa, L. Active Atoms and Interstitials in Two-Dimensional Colloidal Crystals. *Phys. Rev. Lett.* **2018**, *120* (26), 268004.
(137) Solovev, A. A.; Mei, Y.; Schmidt, O. G. Catalytic Microstrider at the Air−Liquid Interface. *Adv. Mater.* **2010**, *22* (39), 4340−4344.
(138) Wang, W.; Giltinan, J.; Zakharchenko, S.; Sitti, M. Dynamic and Programmable Self-Assembly of Micro-Rafts at the Air-Water Interface. *Sci. Adv.* **2017**, *3* (5), No. e1602522.
(139) Nakata, S.; Iguchi, Y.; Ose, S.; Kuboyama, M.; Ishii, T.; Yoshikawa, K. Self-Rotation of a Camphor Scraping on Water: New Insight into the Old Problem. *Langmuir* **1997**, *13* (16), 4454−4458.
(140) Nakata, S.; Nagayama, M.; Kitahata, H.; Suematsu, N. J.; Hasegawa, T. Physicochemical Design and Analysis of Self-Propelled Objects that are Characteristically Sensitive to Environments. *Phys. Chem. Chem. Phys.* **2015**, *17* (16), 10326−10338.
(141) Li, M.; Zhang, H.; Liu, M.; Dong, B. Motion-Based Glucose Sensing Based on a Fish-Like Enzymeless Motor. *J. Mater. Chem. C* **2017**, *5* (18), 4400−4407.
(142) Suematsu, N. J.; Nakata, S. Evolution of Self-Propelled Objects: From the Viewpoint of Nonlinear Science. *Chem. - Eur. J.* **2018**, *24* (24), 6308−6324.
(143) Wang, L.-l.; Chen, L.; Zhang, J.; Duan, J.-m.; Wang, L.; Silber-Li, Z.-h.; Zheng, X.; Cui, H.-h. Efficient Propulsion and Hovering of Bubble-Driven Hollow Micromotors underneath an Air−Liquid Interface. *Langmuir* **2018**, *34* (35), 10426−10433.
(144) Archer, R.; Campbell, A.; Ebbens, S. Glancing Angle Metal Evaporation Synthesis of Catalytic Swimming Janus Colloids with Well Defined Angular Velocity. *Soft Matter* **2015**, *11* (34), 6872−6880.
(145) Wang, X.; In, M.; Blanc, C.; Würger, A.; Nobili, M.; Stocco, A. Janus Colloids Actively Rotating on the Surface of Water. *Langmuir* **2017**, *33* (48), 13766−13773.
(146) Takagi, D.; Braunschweig, A. B.; Zhang, J.; Shelley, M. J. Dispersion of Self-Propelled Rods Undergoing Fluctuation-Driven Flips. *Phys. Rev. Lett.* **2013**, *110* (3), No. 038301.
(147) Zhou, C.; Zhao, L.; Wei, M.; Wang, W. Twists and Turns of Orbiting and Spinning Metallic Microparticles Powered by Megahertz Ultrasound. *ACS Nano* **2017**, *11* (12), 12668−12676.

DOI: 10.1021/acsami.8b13103
ACS Appl. Mater. Interfaces XXXX, XXX, XXX−XXX

(148) Yang, F.; Mou, F.; Jiang, Y.; Luo, M.; Xu, L.; Ma, H.; Guan, J. Flexible Guidance of Microengines by Dynamic Topographical Pathways in Ferrofluids. *ACS Nano* **2018**, *12* (7), 6668−6676.
(149) Palacci, J.; Cottin-Bizonne, C.; Ybert, C.; Bocquet, L. Sedimentation and Effective Temperature of Active Colloidal Suspensions. *Phys. Rev. Lett.* **2010**, *105* (8), No. 088304.
(150) Campbell, A. I.; Wittkowski, R.; Ten Hagen, B.; Löwen, H.; Ebbens, S. J. Helical paths, Gravitaxis, and Separation Phenomena for Mass-Anisotropic Self-Propelling Colloids: Experiment versus Theory. *J. Chem. Phys.* **2017**, *147* (8), No. 084905.
(151) Campbell, A. I.; Ebbens, S. J. Gravitaxis in Spherical Janus Swimming Devices. *Langmuir* **2013**, *29* (46), 14066−14073.
(152) Singh, D. P.; Uspal, W. E.; Popescu, M. N.; Wilson, L. G.; Fischer, P. Photogravitactic Microswimmers. *Adv. Funct. Mater.* **2018**, *28*, 1706660.
(153) Novotny, L.; Bian, R. X.; Xie, X. S. Theory of Nanometric Optical Tweezers. *Phys. Rev. Lett.* **1997**, *79* (4), 645.
(154) Gosse, C.; Croquette, V. Magnetic Tweezers: Micromanipulation and Force Measurement at the Molecular Level. *Biophys. J.* **2002**, *82* (6), 3314−3329.
(155) Fan, D.; Zhu, F.; Cammarata, R.; Chien, C. Electric Tweezers. *Nano Today* **2011**, *6* (4), 339−354.
(156) Zong, Y.; Liu, J.; Liu, R.; Guo, H.; Yang, M.; Li, Z.; Chen, K. An Optically Driven Bistable Janus Rotor with Patterned Metal Coatings. *ACS Nano* **2015**, *9* (11), 10844−10851.
(157) Evander, M.; Nilsson, J. Acoustofluidics 20: Applications in Acoustic Trapping. *Lab Chip* **2012**, *12* (22), 4667−4676.
(158) Guo, F.; Mao, Z.; Chen, Y.; Xie, Z.; Lata, J. P.; Li, P.; Ren, L.; Liu, J.; Yang, J.; Dao, M. Three-Dimensional Manipulation of Single Cells Using Surface Acoustic Waves. *Proc. Natl. Acad. Sci. U. S. A.* **2016**, *113* (6), 1522−1527.
(159) Wang, W.; Duan, W.; Zhang, Z.; Sun, M.; Sen, A.; Mallouk, T. E. A Tale of Two Forces: Simultaneous Chemical and Acoustic Propulsion of Bimetallic Micromotors. *Chem. Commun.* **2015**, *51* (6), 1020−1023.
(160) Takatori, S. C.; De Dier, R.; Vermant, J.; Brady, J. F. Acoustic Trapping of Active Matter. *Nat. Commun.* **2016**, *7*, 10694.
(161) Wang, W.; Castro, L. A.; Hoyos, M.; Mallouk, T. E. Autonomous Motion of Metallic Microrods Propelled by Ultrasound. *ACS Nano* **2012**, *6* (7), 6122−6132.
(162) Rao, K. J.; Li, F.; Meng, L.; Zheng, H.; Cai, F.; Wang, W. A Force to be Reckoned with: A Review of Synthetic Microswimmers Powered by Ultrasound. *Small* **2015**, *11* (24), 2836−2846.
(163) Xu, T.; Xu, L.-P.; Zhang, X. Ultrasound Propulsion of Micro-/Nanomotors. *Appl. Mater. Today* **2017**, *9*, 493−503.
(164) Li, J.; Gao, W.; Dong, R.; Pei, A.; Sattayasamitsathit, S.; Wang, J. Nanomotor Lithography. *Nat. Commun.* **2014**, *5*, 5026.
(165) Lin, X.; Si, T.; Wu, Z.; He, Q. Self-Thermophoretic Motion of Controlled Assembled Micro-/Nanomotors. *Phys. Chem. Chem. Phys.* **2017**, *19* (35), 23606−23613.
(166) Gangwal, S.; Cayre, O. J.; Bazant, M. Z.; Velev, O. D. Induced-Charge Electrophoresis of Metallodielectric Particles. *Phys. Rev. Lett.* **2008**, *100* (5), No. 058302.
(167) Yan, J.; Han, M.; Zhang, J.; Xu, C.; Luijten, E.; Granick, S. Reconfiguring Active Particles by Electrostatic Imbalance. *Nat. Mater.* **2016**, *15* (10), 1095.
(168) Fournier-Bidoz, S.; Arsenault, A. C.; Manners, I.; Ozin, G. A. Synthetic Self-Propelled Nanorotors. *Chem. Commun.* **2005**, No. 4, 441−443.

DOI: 10.1021/acsami.8b13103
ACS Appl. Mater. Interfaces XXXX, XXX, XXX−XXX